







ORIGINAL RESEARCH

Endothelial Foxp1 Regulates Neointimal Hyperplasia Via Matrix Metalloproteinase-9/Cyclin Dependent Kinase Inhibitor 1B Signal Pathway

Xiaoli Chen, MD*; Jianfei Xu, MD*; Wenzhen Bao, MD*; Hongda Li, MD; Wenrun Wu , MD; Jiwen Liu, MD, PhD; Jingjiang Pi, MD, PhD; Brian Tomlinson , MD; Paul Chan , MD; Chengchao Ruan , PhD; Qi Zhang, MD, PhD; Lin Zhang, MD, PhD; Huimin Fan, MD, PhD; Edward Morrissey, PhD; Zhongmin Liu, MD, PhD; Yuzhen Zhang, MD, PhD; Li Lin, MD, PhD; Jie Liu , PhD; Tao Zhuang , PhD

BACKGROUND: The endothelium is essential for maintaining vascular physiological homeostasis and the endothelial injury leads to the neointimal hyperplasia because of the excessive proliferation of vascular smooth muscle cells. Endothelial Foxp1 (forkhead box P1) has been shown to control endothelial cell (EC) proliferation and migration in vitro. However, whether EC-Foxp1 participates in neointimal formation in vivo is not clear. Our study aimed to investigate the roles and mechanisms of EC-Foxp1 in neointimal hyperplasia.

METHODS AND RESULTS: The wire injury femoral artery neointimal hyperplasia model was performed in Foxp1 EC-specific loss-of-function and gain-of-function mice. EC-Foxp1 deletion mice displayed the increased neointimal formation through elevation of vascular smooth muscle cell proliferation and migration, and the reduction of EC proliferation hence reendothelialization after injury. In contrast, EC-Foxp1 overexpression inhibited the neointimal formation. EC-Foxp1 paracrine regulated vascular smooth muscle cell proliferation and migration via targeting matrix metalloproteinase-9. Also, EC-Foxp1 deletion impaired EC repair through reduction of EC proliferation via increasing cyclin dependent kinase inhibitor 1B expression. Delivery of cyclin dependent kinase inhibitor 1B-siRNA to ECs using RGD (Arg-Gly-Asp)-peptide magnetic nanoparticle normalized the EC-Foxp1 deletion-mediated impaired EC repair and attenuated the neointimal formation. EC-Foxp1 regulates matrix metalloproteinase-9/cyclin dependent kinase inhibitor 1B signaling pathway to control injury induced neointimal formation.

CONCLUSIONS: Our study reveals that targeting EC-Foxp1-matrix metalloproteinase-9/cyclin dependent kinase inhibitor 1B pathway might provide future novel therapeutic interventions for restenosis.

Key Words: cyclin dependent kinase inhibitor 1B (Cdkn1b) ■ matrix metalloproteinase-9 (MMP9) ■ neointimal formation ■ transcription factor forkhead box protein P1 (Foxp1)

Correspondence to: Tao Zhuang, PhD, Key Laboratory of Arrhythmias of the Ministry of Education of China, Research Center for Translational Medicine, Shanghai East Hospital, Tongji University School of Medicine, 150 Jimo Rd, Pudong New District, Shanghai 200120, China. Email: zhuangtao5217@163.com and Department of Physiology and Pathophysiology, School of Basic Medical Sciences, Fudan University, 131 Dong'an Rd, Xuhui District, Shanghai 200032, China. Email: zhuangtao5217@163.com or Jie Liu, PhD, Key Laboratory of Arrhythmias of the Ministry of Education of China, Research Center for Translational Medicine, Shanghai East Hospital, Tongji University School of Medicine, 150 Jimo Rd, Pudong New District, Shanghai 200120, China. Email: kenliujie@126.com or Li Lin, MD, PhD, Department of Cardiology, Shanghai East Hospital, Tongji University School of Medicine, 150 Jimo Rd, Pudong New District, Shanghai 200120, China. Email: linli777@126.com

*X. Chen, J. Xu, and W. Bao contributed equally.

Supplemental Material is available at <https://www.ahajournals.org/doi/suppl/10.1161/JAHA.122.026378>

For Sources of Funding and Disclosures, see page 13.

© 2022 The Authors. Published on behalf of the American Heart Association, Inc., by Wiley. This is an open access article under the terms of the [Creative Commons Attribution-NonCommercial-NoDerivs](https://creativecommons.org/licenses/by-nc-nd/4.0/) License, which permits use and distribution in any medium, provided the original work is properly cited, the use is non-commercial and no modifications or adaptations are made.

JAHA is available at: www.ahajournals.org/journal/jaha

CLINICAL PERSPECTIVE

What Is New?

- Endothelial-specific knockout of Foxp1 (forkhead box P1) increases neointimal formation after injury, and endothelial Foxp1 overexpression inhibits neointimal formation.
- EC (endothelial cell)-Foxp1 paracrine regulates vascular smooth muscle cell proliferation and migration via targeting matrix metalloproteinase-9.
- EC-Foxp1 deletion impaired EC repair through reduction of EC proliferation via increasing cyclin dependent kinase inhibitor 1B expression.

What Are the Clinical Implications?

- Percutaneous coronary intervention causes injury to the vascular endothelium leading to incomplete reendothelialization that is usually dysfunctional, and which stimulates the proliferation and migration of smooth muscle cells, thereby promoting neointimal hyperplasia.
- EC-Foxp1-matrix metalloproteinase-9/cyclin dependent kinase inhibitor 1B pathway has the potential to provide future novel therapeutic interventions for restenosis.

Nonstandard Abbreviations and Acronyms

Cdkn1b	cyclin dependent kinase inhibitor 1B
ECs	endothelial cells
Foxp1	Forkhead box P1
HUVECs	human umbilical vein endothelial cells
MMP9	matrix metalloproteinase-9
RT-qPCR	real-time quantitative reverse transcription polymerase chain reaction
VSMCs	vascular smooth muscle cells

Percutaneous coronary intervention (PCI) is now a well-established treatment for coronary artery disease, which is the major cause of mortality worldwide.^{1,2} However, restenosis remains a fundamental complication of any percutaneous intervention and although stenting dramatically reduces restenosis, it does not entirely eliminate it. Management of patients with in-stent restenosis remains an important clinical problem.

The pathophysiologic mechanism of restenosis is heterogeneous and mainly attributed to the aggressive neointimal proliferation from dysregulation of endothelial cells (ECs) and excess vascular smooth muscle cell (VSMC) proliferation and migration.³⁻⁶ Because ECs

play an important role in the proliferation and migration of VSMC in the process of intimal hyperplasia, the cellular and molecular pathways that regulate this process are needed to further investigated.

The healthy endothelium communicates with the underlying VSMCs to control the homeostasis of mature vessels.^{6,7} PCI-induced vascular injury results in the release of growth factors, cytokines by activated endothelium, which stimulates the aberrant proliferation and migration of smooth muscle cells (SMCs), and then leads to the formation of neointima and restenosis.^{4,6,8,9} Our previous study showed that endothelial GATA zinc finger transcription factor family-6 transcriptionally regulated platelet-derived growth factor-B expression to control VSMC proliferation and migration in a paracrine manner contributing to neointimal formation,¹⁰ which further corroborate the importance of EC-VSMC communications.

PCI stent deployment damaged the vascular endothelium and caused the repopulation of the denuded regions from adjacent ECs.^{11,12} The incomplete reendothelialization or the regenerated endothelium might have impaired function promoting in-stent restenosis.^{7,8,11,12} The drug-eluting stents efficiently inhibit neointimal hyperplasia through decreasing cell proliferation, but also restrain reendothelialization of the vessel where the stent is deployed, hence leading to late in-stent restenosis and thrombosis events. A study reported that increase of endothelial proliferation or reendothelialization after injury correlated with the diminished intimal hyperplasia.¹³ However, the molecular mechanisms regulating reendothelialization and the function of repaired endothelium are incompletely understood.

Foxps (forkhead box proteins P) are large modular transcription repressors that bind to a motif sequence (5'-TRTTTRY-3') on the target gene.^{14,15} Foxp1 is highly expressed in vascular ECs and our previous study showed Foxp1 expression in endocardium repressed Sox17 expression, which, through regulation of b-catenin activity, controlled Fgf16/20 expression and influenced cardiomyocyte proliferation, and further ventricular myocardial development.¹⁶ Our recent study reported that Foxp1 repressed endothelial transforming growth factor- β signals to inhibit fibroblast proliferation and transformation to myofibroblasts, and further attenuated pathological cardiac remodeling and improved cardiac function.¹⁷ Therefore, we hypothesize that Foxp1 might regulate endothelial function to control VSMC phenotypic change and influence wire injury EC denuded induced neointimal formation. Also, Foxp1 was reported to be essential for endothelial angiogenic function and silencing of Foxp1 in vitro resulted in inhibition of proliferation, tube formation, and migration of cultured ECs.¹⁸ Hence, we explored the roles and mechanisms of Foxp1 in injury-induced reendothelialization for neointimal formation in vivo.

Our study found that Foxp1 deletion in ECs resulted in significant increase of VSMC proliferation/migration and neointimal formation upon wire injury and we identified matrix metalloproteinase-9 (MMP9) as a Foxp1 direct target gene, and the EC-Foxp1-MMP9 pathway regulated VSMC proliferation and migration. Also, EC-Foxp1 deletion mice exhibited a significant decrease of reendothelialization following femoral artery injury, and a cell cycle regulating gene, cyclin dependent kinase inhibitor 1B (Cdkn1b), was identified as the Foxp1 target gene. Delivery of Cdkn1b-siRNA using RGD (Arg-Gly-Asp)-peptide magnetic nanoparticle with high endothelial cell affinity reversed the EC-Foxp1 deletion-mediated impaired EC repair and attenuated the neointimal formation. Contrary to EC-Foxp1 loss-of-function mice, EC-Foxp1 gain-of-function mice were protected against neointimal hyperplasia with increase of EC proliferation and decrease of VSMC proliferation and migration. The results of this study expand our understanding of wire injury EC denudation induced neointimal hyperplasia and will help to identify potential therapeutic targets of endothelial signals for future therapeutic interventions for restenosis.

METHODS

The data that support the findings of this study are available from the corresponding author upon reasonable request. See Data S1 for detailed Materials and Methods.

Animals

All animal procedures were approved by the Institutional Animal Care and Use Committee at Tongji University. The conditional Foxp1 loss-of-function (*Foxp1^{fllox/fllox}*)¹⁶ and gain-of-function mice¹⁹ were crossed with tamoxifen-inducible *Cdh5* promoter-driven Cre line (*Cdh5-Cre^{ERT2}*)²⁰ to generate EC-specific Foxp1 loss- and gain-of-function mice, *Foxp1^{ECKO}* and *Foxp1^{ECTg}* mice. Wire injury-induced femoral arterial neointima formation mouse model was performed with a detailed description in Data S1. Details of lentiviral-MMP9-shRNA infection in vivo and delivery of Cdkn1b-siRNA to endothelial cells using RGD (Arg-Gly-Asp)-peptide magnetic nanoparticle, hematoxylin and eosin staining, and immunostaining, were also provided in Data S1.

Molecular Methods

The details of real-time quantitative reverse transcription polymerase chain reaction (RT-qPCR), immunoblotting, expression vectors, cell culture/transfection and proliferation/migration assay, lentiviral package, isolation of mouse lung endothelial cells, RNA high-throughput sequencing methods were provided in

Data S1, as well as chromatin immunoprecipitation assay, and luciferase reporter assay.

Statistical Analysis

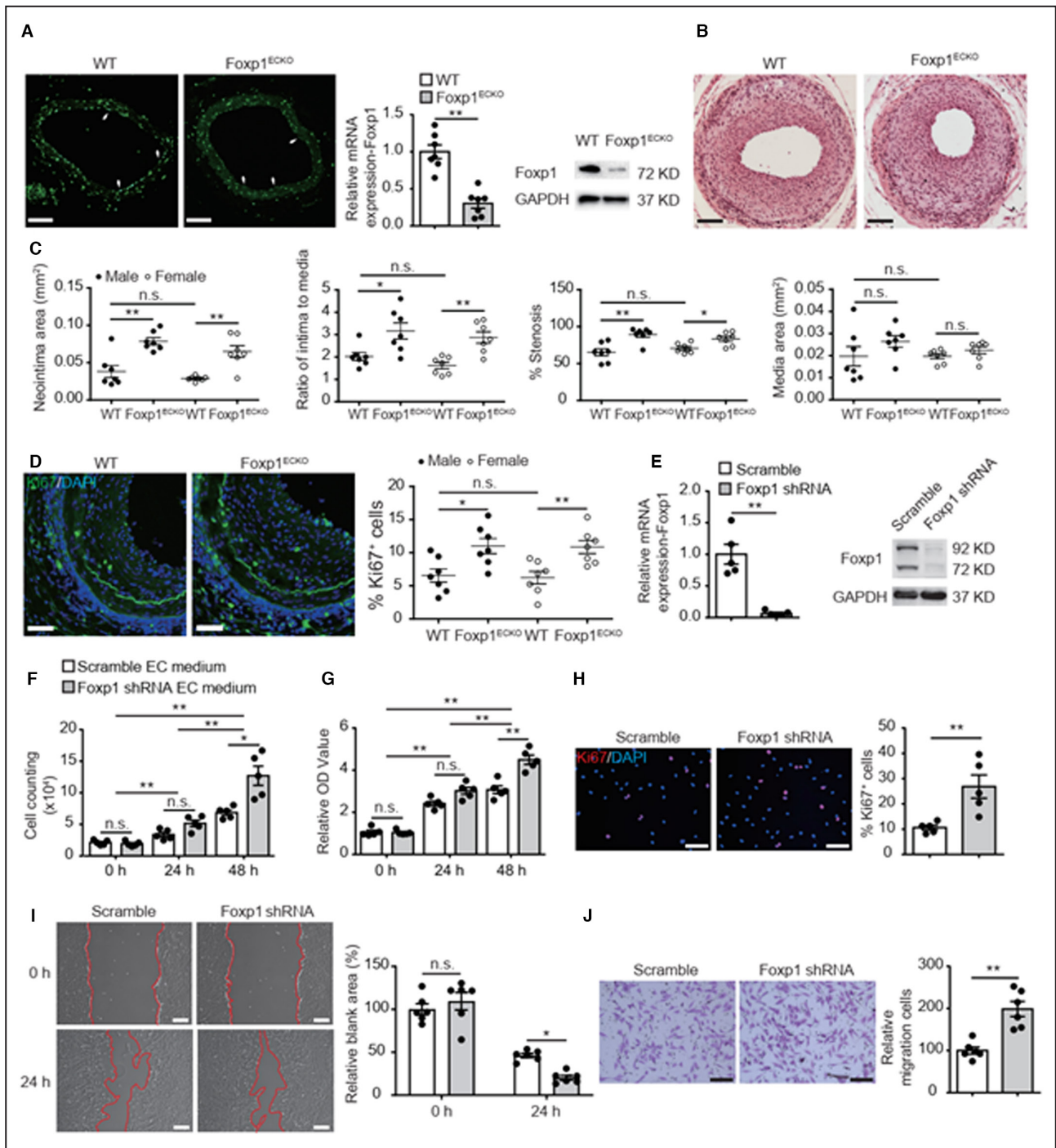
Continuous variables were presented as mean±SEM, and the statistical analysis was performed using SPSS 16.0 Statistics. Unpaired 2-tailed Student *t*-test was used for comparisons between 2 groups, and 1-way ANOVA followed by the post-hoc Tukey multiple comparison analysis for multiple groups. Two-way repeated-measures ANOVA was used for comparisons between multiple groups when there were 2 experimental factors. *P*<0.05 means statistically significant.

RESULTS

Genetic Inhibition of Foxp1 in Endothelium Promotes Neointimal Formation Following Injury through Increase of VSMC Proliferation and Migration

Vascular endothelial dysfunction plays a vital role in the pathogenesis of vascular diseases including neointimal thickening and atherosclerosis. EC activation was reported to be associated with reduced Foxp1-dependent transcriptional activation.^{17,21–23} We found a 54% reduction of Foxp1 expression in endothelium of injured femoral arteries by RT-qPCR (*P*=0.0252) (Figure S1A). Immunostaining on injured femoral arteries also confirmed the decrease of Foxp1 expression in endothelium (Figure S1B). These data indicated that endothelial Foxp1 (EC-Foxp1) might participate in wire-injury induced neointimal formation. To confirm the role of EC-Foxp1 in neointimal formation after wire injury, EC-Foxp1 deletion mice (*Foxp1^{ECKO}*) were generated and RT-qPCR demonstrated 70% reduction in Foxp1 mRNA level in ECs from *Foxp1^{ECKO}* mice (*P*=0.001), which was further confirmed by immunostaining and Western blot (Figure 1A).

Specific deletion of Foxp1 in ECs caused significantly increased neointimal area from 0.03±0.004 μm² in wild-type (WT) mice (mean±SEM) to 0.07±0.005 μm² in *Foxp1^{ECKO}* mice (*P*=0.001), intima-to-media ratio from 1.8±0.1 to 3.0±0.2 (*P*=0.001) and percentage of stenosis from 68.0±2.7% to 86.3±2.5% (*P*=0.001) without change of media area from 0.02±0.002 μm² to 1.8±0.1 μm² (*P*>0.05) at day 28 after wire injury of femoral artery, and no sex difference was observed in the process of neointimal formation (Figure 1B and 1C). Significantly increased proliferation was observed in the neointima of *Foxp1^{ECKO}* mice by Ki67 immunostaining (*Foxp1^{ECKO}* versus WT: 10.9±0.7% versus 6.4±0.7%; *P*=0.001) (Figure 1D). Because the injury-induced neointima is mainly composed of VSMCs,²⁴ the result suggested that the increased neointimal



formation in *Foxp1^{EKO}* mice after injury was attributable to the increase of VSMC proliferation.

To further confirm the *in vivo* findings, we then knockdown Foxp1 in cultured human umbilical vein endothelial cells (HUVECs) and investigated the effects of EC-Foxp1 on VSMC proliferation and migration. Foxp1 expression was reduced by 99% in HUVECs treated with Foxp1 shRNA (Figure 1E). The effect of Foxp1 knockdown in HUVECs on cell proliferation of human aortic smooth muscle cells was determined by cell counting, 3-(4, 5-dimethylthiazol-2-yl)-2,

5-diphenyltetrazolium bromide (MTT) assay, and Ki67 staining assay (Figure 1F through Figure 1H). SMCs incubated with scramble EC medium increased cell number from $2.1 \pm 0.2 \times 10^4$ at 0 hours to $3.4 \pm 0.4 \times 10^4$ ($P=0.006$) at 24 hours and $6.9 \pm 0.4 \times 10^4$ ($P=0.001$) at 48 hours, with significant increase of cell number between 24 and 48 hours ($P=0.001$). SMCs treated with Foxp1 shRNA EC medium also increased cell number from 1.9×10^4 at 0 hours to 5.2×10^4 ($P=0.002$) at 24 hours and 12.7×10^4 ($P=0.003$) at 48 hours, with significant difference between 24 and 48 hours ($P=0.005$).

Figure 1. Genetic deletion of endothelial cell (EC)-Foxp1 (forkhead box P1) increases neointimal formation through promoting vascular smooth muscle cell proliferation and migration.

A, Foxp1 immunostaining (left) in femoral artery, real-time quantitative reverse transcription polymerase chain reaction (middle) and Western blot (right) in vascular ECs of EC-Foxp1 deletion mice (*Foxp1^{ECKO}*, *Foxp1^{fllox/fllox};Cdh5Cre^{ERT2}*) and wild-type mice (n=7). White arrowheads indicating Foxp1 staining in ECs. **B** and **C**, *Foxp1^{ECKO}* mutant mice of both male and female sex exhibit increased neointimal formation at 28 days after femoral artery wire injury compared with wild-type littermate mice, with representative images (B) and quantification of neointima area, intima to media ratio, percentage stenosis and media area (C) (n=7 females/7 males for each group). **D**, *Foxp1^{ECKO}* mutant mice exhibit significantly increased cell proliferation in the neointima by Ki67 immunostaining, with representative images (left) and quantification data (right) (n=7 females/7 males for each group). **E**, Significant reduction of Foxp1 expression in human umbilical vein ECs treated with lentiviral Foxp1-shRNA is confirmed by real-time quantitative reverse transcription (left) and Western blot (right) compared with human umbilical vein ECs with control scramble-shRNA (n=5). **F** through **H**, Condition medium from Foxp1 knockdown human umbilical vein ECs significantly increases human aortic smooth muscle cell proliferation assessed by cell counting (F), 3-(4, 5-dimethylthiazol-2-yl)-2, 5-diphenyltetrazolium bromide (G), and Ki67 staining with quantification of Ki67-positive cells on the right (H) (n=5). Statistical values of cell counting and 3-(4, 5-dimethylthiazol-2-yl)-2, 5-diphenyltetrazolium bromide are shown in Data S2. **I** and **J**, Condition medium from Foxp1 knockdown human umbilical vein endothelial cells significantly increases human aortic smooth muscle cell migration shown by wound healing (I) and transwell assay (J) with representative images (left) and quantification (right) (n=6). Data are means±SEM. EC indicates endothelial cell; Foxp1, forkhead box P1; OD, optical density; and WT, wild-type. **P*<0.05, ***P*<0.01. Scale bars: A=50 μm, B, D, H, I, J=100 μm.

We further found a significant increase in cell number between scramble EC medium and Foxp1 shRNA EC medium at 48 hours (*P*=0.049) (Figure 1F). Similarly, the relative MTT activity (MTT activity divided by that at 0 hours) of SMCs incubated with scramble EC medium was 2.4±0.1 (*P*=0.001) at 24 hours and 3.1±0.2 (*P*=0.001) at 48 hours, with significant increase of cell number between 24 and 48 hours (*P*=0.002). While the relative MTT activity of SMCs after Foxp1 shRNA EC medium treatment was 3.0±0.2 (*P*=0.001) at 24 hours and 4.5±0.2 (*P*=0.001) at 48 hours, with significant increase of cell number between 24 and 48 hours (*P*=0.001). MTT activity of SMCs incubated with Foxp1 shRNA EC medium was higher than that with scramble EC medium at 48 hours (*P*=0.004) (Figure 1G). Ki67 staining assay showed an increase in the percentage of Ki67⁺ SMCs treated with Foxp1 shRNA EC medium (26.9±4.6%) compared with SMCs treated with scramble EC medium (10.6±0.9%; *P*=0.009). In addition to increased VSMC proliferation, we found that the condition medium of Foxp1 knockdown HUVECs promoted human aortic smooth muscle cell migration shown by wound healing (Relative blank area: Foxp1 shRNA 20.2±2.6 versus scramble shRNA 46.2±2.5 at 24 hours after wounding; *P*=0.017) and transwell chemotactic assay (Foxp1 shRNA 198.7±18.0 versus scramble shRNA 100.1±8.3; *P*=0.001) (Figure 1I and 1J). These data suggest that EC-Foxp1 deficiency increases VSMC proliferation and migration contributing to the increase of neointimal hyperplasia in vivo.

EC-Foxp1 Regulates VSMC Proliferation and Migration and Neointimal Formation Via Regulating MMP9 Expression

To explore the downstream mechanisms by which EC-Foxp1 affected injury-induced neointimal hyperplasia, we performed RNA sequencing with ECs from Foxp1 deletion and littermate control WT mice was

performed as previous described.²¹ RT-qPCR showed 2-fold increase of matrix metalloproteinase (MMP)-9 expression in endothelium after femoral artery injury (*P*=0.001) (Figure S1C), which was confirmed by Immunostaining (Figure S1D). Foxp1 deletion in EC further increased MMP9 expression shown by RNA sequencing (2-fold increase; *P*=0.001) (Figure 2A) and Western blot (Figure 2B). Moreover, we found an increased activity of EC-MMP9 from 20.5±3.4 in WT mice to 58.2±6.2 in *Foxp1^{ECKO}* mutant mice (*P*=0.001) (Figure 2C).

To validate the regulatory role of Foxp1 on MMP9 expression, we performed chromatin immunoprecipitation assays in mouse lung ECs and found that Foxp1 bound to the mouse MMP9 promoter (Figure 2D). There are 6 Foxp1 binding sites in the promoter region from -4.0 kb to -3.5 kb before the translational starting site of the MMP9 gene (Figure S2A) and luciferase reporter assay showed that Foxp1 overexpression repressed the luciferase activity in a dose-dependent manner (Figure 2E and Figure S2B).

Previous studies reported that activation of MMP9 was involved in SMC proliferation and migration contributing to neointimal formation.^{25–27} To clarify whether the EC-Foxp1-MMP9 pathway regulates VSMC proliferation and migration, we constructed a lentiviral MMP9 shRNA vector and applied this lenti-MMP9 shRNA to *Foxp1^{ECKO}* mice and the littermate WT control mice attempting to rescue the EC-Foxp1 deficiency-mediated increased neointimal hyperplasia phenotypes. 73.4% MMP9 reduction was observed in femoral artery treated with lenti-MMP9 shRNA by qPCR, which was confirmed by Western blotting (Figure 2F). MMP9 knockdown by lenti-MMP9 shRNA inhibited wire injury induced neointimal hyperplasia shown by decreased neointima area (MMP9 shRNA 1.6±0.2 μm² versus scramble shRNA 1.3±0.1 μm²; *P*>0.05), intima-to-media ratio (MMP9 shRNA 2.9±0.3 versus scramble shRNA 2.1±0.2; *P*>0.05) and percent of stenosis (MMP9

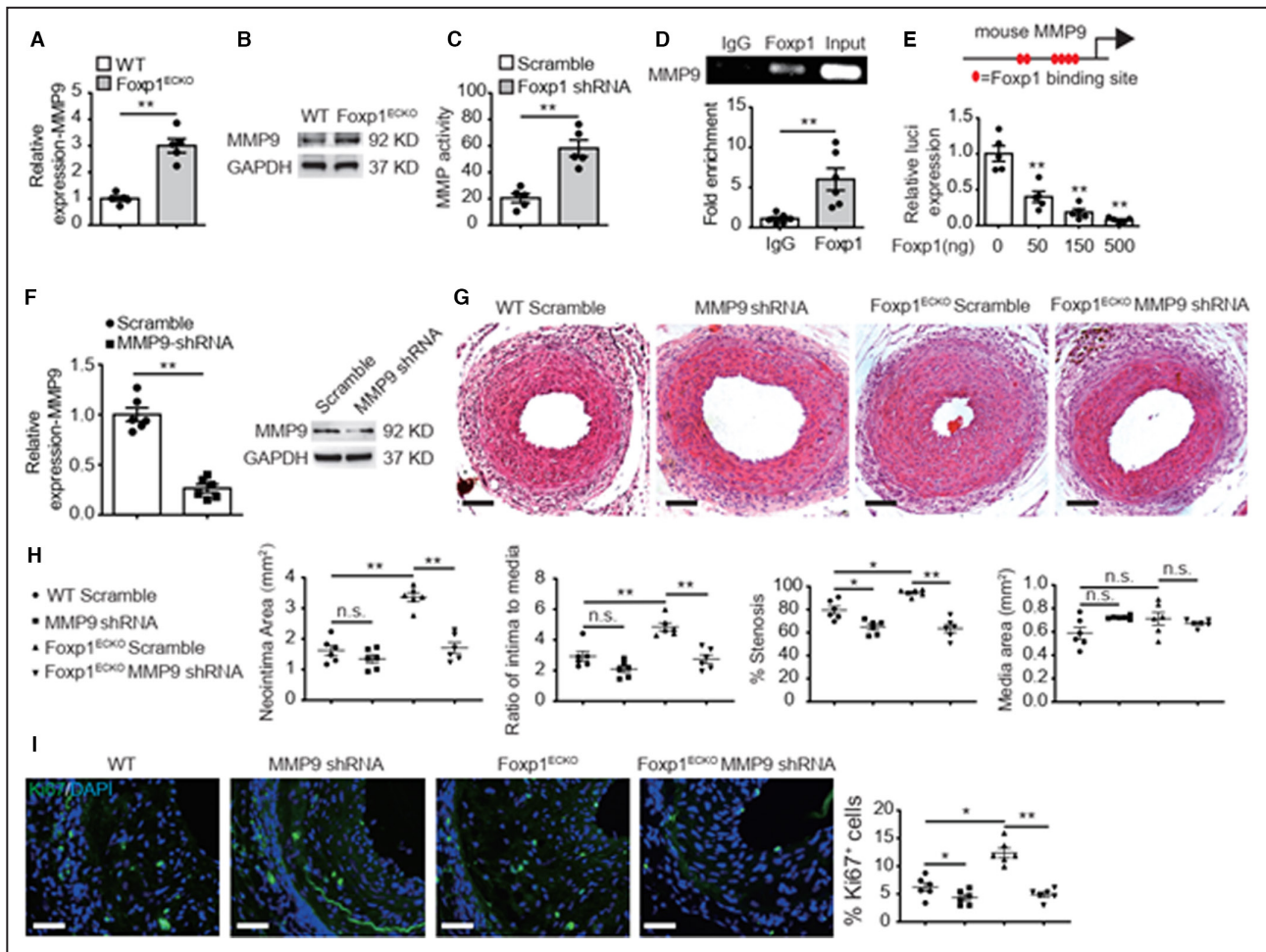


Figure 2. Foxp1 directly regulate matrix metalloproteinase-9 (MMP9) gene expression in endothelial cells (ECs) and in vivo MMP9 inhibition reverses the enhanced neointimal formation.

A through **C**, *Foxp1*^{EKO} mutant mice exhibit increased expression and activity of MMP9 shown by real-time quantitative reverse transcription polymerase chain reaction (A), Western blot (B), and MMP activity assay (C) in vascular ECs compared with wild-type littermates (n=5). **D**, Chromatin immunoprecipitation assay shows that Foxp1 binds to the mouse MMP9 promoter by quantitative polymerase chain reaction and in agarose gel (n=6). **E**, The promoter region of MMP9, -4.0 kb to -3.5 kb before ATG translational site has 6 Foxp1 binding sites (left) and luciferase assay shows that Foxp1 expression vector dose-dependent suppresses the luciferase reporter activity of this MMP9 promoter region (right) (n=5). **F**, Real-time quantitative reverse transcription polymerase chain reaction and Western blot confirms the decreased expression of MMP9 in wire-injured femoral artery after application of lentiviral MMP9-shRNA compared with lentiviral scramble-shRNA (n=6). **G** and **H**, MMP9 knockdown reverses the increased neointimal formation at 28 days after femoral artery wire injury caused by EC-Foxp1 deletion, with representative images (G) and quantification of neointima area, intima-to-media ratio, percentage stenosis and media area (H) (n=6 for each group). **I**, MMP9 knockdown reverses EC-Foxp1 deletion mediated increase of Ki67-positive cells in neointima at 28 days after femoral artery wire injury, with representative images (left) and quantification data (right) (n=6 for each group). Data are means±SEM. EC indicates endothelial cell; Foxp1, forkhead box P1; IgG, immunoglobulin G; MMP9, matrix metalloproteinase-9; OD, optical density; and WT, wild-type. **P*<0.05, ***P*<0.01. Scale bars: G, I=100 μm.

shRNA 79.6±3.4% versus scramble shRNA 64.8±2.5%; *P*=0.007). Immunostaining showed that MMP9 knockdown decreased the increased Ki67-positive cells in the neointima of mice from 6.2±0.7% to 4.4±0.5% (*P*>0.05). Furthermore, MMP9 knockdown significantly reversed the increased neointimal hyperplasia in *Foxp1*^{EKO} mutant mice as shown by reversal of the increased neointimal area (MMP9 shRNA 1.7±0.2 μm² versus scramble shRNA 3.4±0.1 μm²; *P*=0.001), intima-to-media ratio (MMP9 shRNA 2.7±0.3 versus scramble

shRNA 4.9±0.2 μm²; *P*=0.025) and percent of stenosis (MMP9 shRNA 63.5±3.5% versus scramble shRNA 94.7±1.2% μm²; *P*=0.001) in the femoral artery wire injury model compared with the scramble shRNA vector control (Figure 2G and 2H). MMP9 knockdown also reversed the increased Ki67-positive cells in the neointima of *Foxp1*^{EKO} mutant mice from 12.4±0.9% to 4.9±0.4% (*P*=0.001) (Figure 2I), suggesting that the EC-Foxp1-MMP9 signal might regulate VSMC proliferation and control in vivo neointimal formation.

We next used the constructed lentiviral MMP9 shRNA vector to investigate the role of MMP9 from ECs in VSMC proliferation and migration. RT-qPCR analysis demonstrated >90% MMP9 expression decrease in lentiviral MMP9 shRNA infected HUVECs ($P=0.001$), which was confirmed by Western blot (Figure 3A). Consistent with in vivo results, MMP9 knockdown in HUVECs decreased SMC proliferation assessed by cell counting ($9.1\pm 0.6\times 10^4$ to $5.6\pm 0.5\times 10^4$; $P=0.008$ at

48 hours), MTT assay (1.5 ± 0.06 to 1.3 ± 0.04 at 24 hours; $P=0.015$, 3.1 ± 0.2 to 2.0 ± 0.1 at 48 hours; $P=0.015$) and Ki67 staining assay ($18.7\pm 1.0\%$ to $9.5\pm 1.2\%$; $P=0.001$), and migration assessed by wound healing (54.3 ± 2.6 to 74.3 ± 3.0 ; $P=0.001$) and transwell chemotactic assay (100.0 ± 5.6 to 57.2 ± 7.0 ; $P=0.017$). Moreover, the condition medium from lentiviral MMP9 shRNA-infected HUVECs significantly reversed the EC-Foxp1 knockdown induced increased SMC proliferation

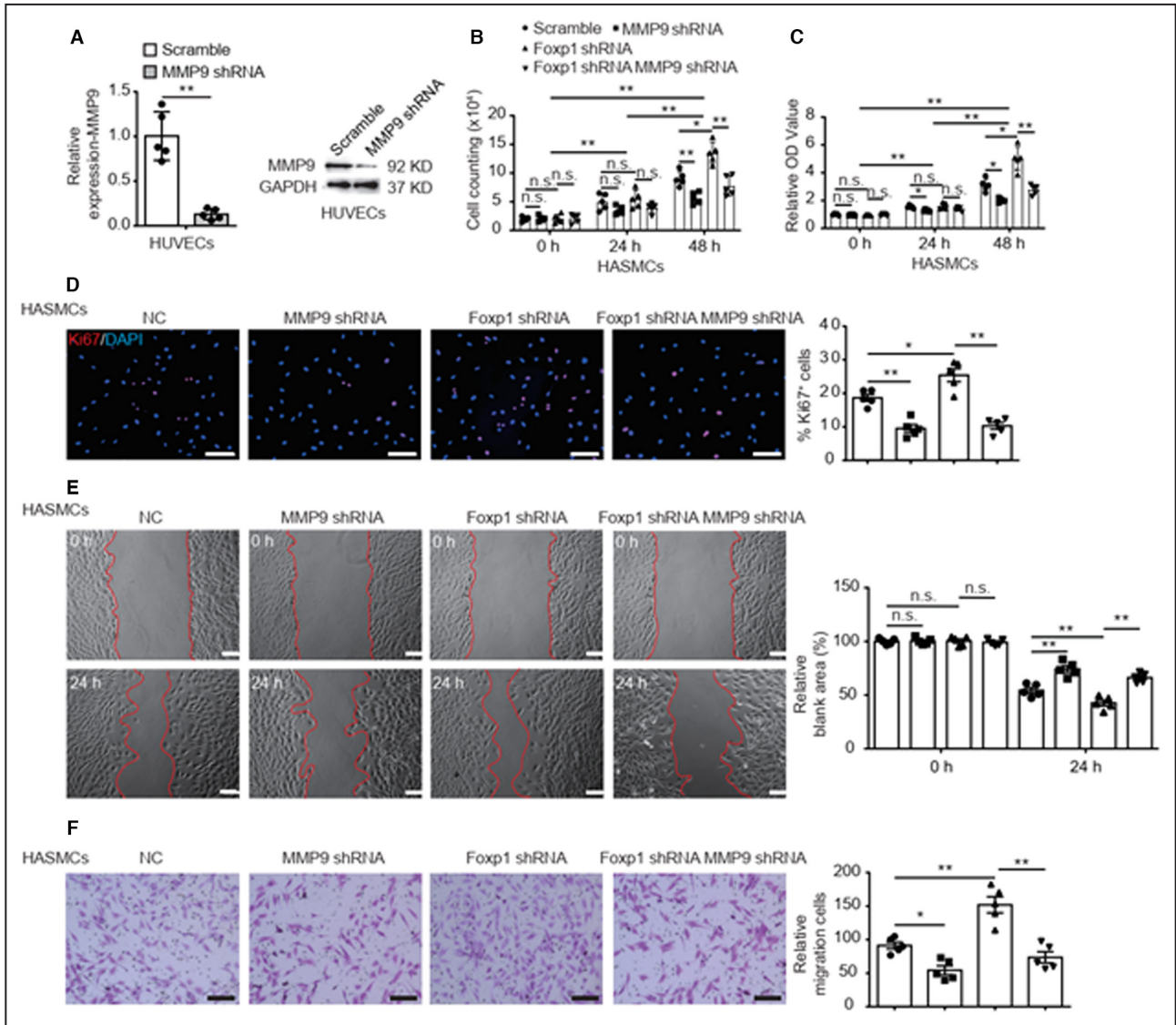


Figure 3. Endothelial matrix metalloproteinase-9 (MMP9) knockdown reverses Foxp1 knockdown-mediated increased vascular smooth muscle cell proliferation and migration in a paracrine manner.

A, MMP9 expression is significantly decreased in human umbilical vein endothelial cells treated with lentiviral MMP9-shRNA compared with lentiviral scramble-shRNA by real-time quantitative reverse transcription polymerase chain reaction (left) and Western blot (right) ($n=5$). **B through D**, The condition medium of human umbilical vein endothelial cells treated with lentiviral MMP9-shRNA reverses the Foxp1 knockdown-mediated increase of vascular smooth muscle cell proliferation in comparison with that of human umbilical vein endothelial cells treated with lentiviral scramble-shRNA, shown by cell counting (B), 3-(4, 5-dimethylthiazol-2-yl)-2, 5-diphenyltetrazolium bromide assay (C) and Ki67 staining with quantification on the right (D) ($n=5$). Statistical values of cell counting and MTT are shown in Data S2. **E and F**, Knockdown MMP9 in human umbilical vein endothelial cells reverses the Foxp1 knockdown mediated increase of vascular smooth muscle cell migration, shown by wound healing (E) and transwell assay (F), with representative images (left) and quantification data (right) ($n=5$). Data are means \pm SEM. Foxp1 indicates forkhead box P1; HASMCs, human aortic smooth muscle cells; MMP9, matrix metalloproteinase-9; and NC, negative control. * $P < 0.05$, ** $P < 0.01$. Scale bars: D, E, F=100 μ m.

(Figure 3B through 3D) by cell counting ($13.5 \pm 0.8 \times 10^4$ to $7.8 \pm 0.8 \times 10^4$ at 48 hours; $P=0.005$), MTT assay (5.0 ± 0.4 to 2.8 ± 0.2 at 48 hours; $P=0.008$) and Ki67 staining assay ($25.4 \pm 1.9\%$ to $10.3 \pm 1.0\%$; $P=0.001$). MMP9 knockdown in HUVECs also reversed the EC-Foxp1 knockdown mediated increase in migration by wound healing (42.6 ± 2.7 to 66.1 ± 1.9 ; $P=0.001$) and transwell chemotactic assay (160.0 ± 12.5 to 77.6 ± 8.6 ; $P=0.001$) (Figure 3E and 3F). These data suggest that Foxp1 deletion in EC regulates MMP9 resulting in the attenuated VSMC proliferation and migration and in vivo neointimal formation.

Endothelial Foxp1 Deletion Impairs Endothelial Repair and Enhances Wire Injury Induced Neointimal Formation

The impaired endothelium results in neointimal thickening following PCI treatment and the improvement of endothelial repair was correlated with the diminished intimal hyperplasia induced by endothelial denudation.^{28,29} Therefore, we studied the effects of EC-Foxp1 on reendothelialization contributing to the injury-induced neointimal hyperplasia. We found an impaired endothelial repair in *Foxp1^{ECKO}* mutant mice ($50.6 \pm 3.7\%$) at day 7 after femoral artery injury compared with WT mice ($63.2 \pm 3.0\%$; $P=0.024$) assessed by Evans blue staining (Figure 4A). Consistent with the in vivo findings, a significant decrease of cell proliferation shown by cell counting (from $10.1 \pm 0.6 \times 10^4$ to $5.5 \pm 0.5 \times 10^4$ at 48 hours; $P=0.029$), MTT assay (from 2.4 ± 0.1 to 1.8 ± 0.1 at 48 hours; $P=0.040$), and Ki67 staining (from 16.3 ± 1.3 to 10.8 ± 1.1 ; $P=0.012$) (Figure 4B through 4D) and attenuation of cell migration shown by wound healing (from 38.1 ± 2.8 to 50.6 ± 2.2 ;

$P=0.049$) and transwell chemotactic assay (from $100 \pm 2.4\%$ to $77.5 \pm 2.3\%$; $P=0.001$) (Figure S3A and S3B) were observed in Foxp1 knockdown HUVECs. These data highlight that EC-Foxp1 deletion impairs EC repair after wire injury by decrease of EC proliferation and migration, therefore aggravates the injury-induced neointimal formation.

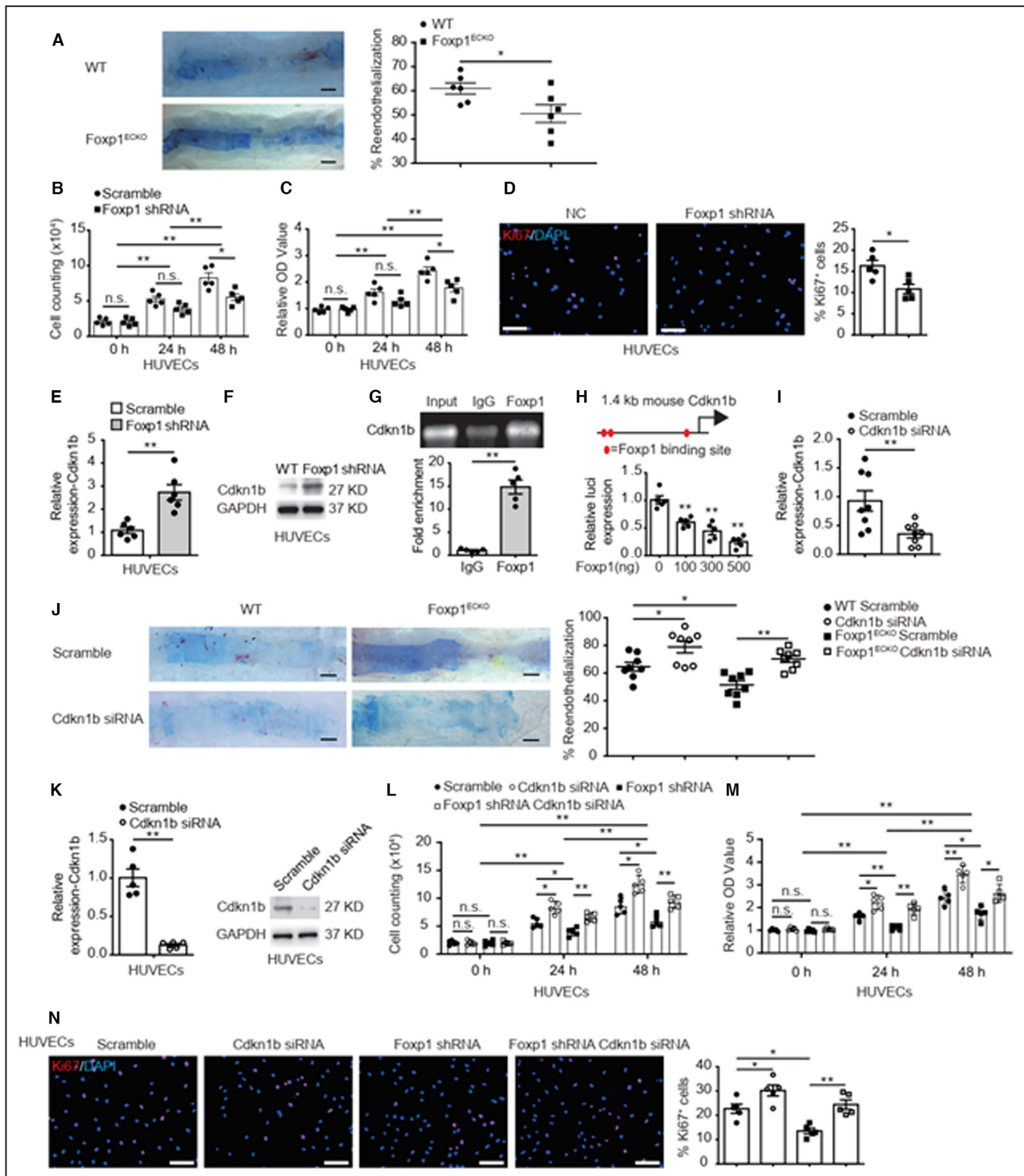
EC-Foxp1 Regulates Endothelial Repair After Injury Denudation and Control Neointimal Formation Via Targeting Cdkn1b Gene Expression

FOX proteins play vital roles in cell cycle progression, proliferation, and differentiation.³⁰ We found a 1.7-fold increased expression of Cdkn1b in HUVECs upon Foxp1 knockdown by RT-qPCR ($P=0.001$) (Figure 4E), which was confirmed by Western blot (Figure 4F). We analyzed the promoter of the Cdkn1b gene and found multiple Foxp1 binding sites (Figure S4A and S4B). Further chromatin immunoprecipitation assays confirmed that Foxp1 directly bound to the Cdkn1b promoter (Figure 4G). We next cloned the promoter region from -1.4 kb to -0.2 kb before exon 1 of the Cdkn1b gene into pGL3 promoter luciferase reporter vector and luciferase reporter assay showed that Foxp1 expression dose-dependent repressed the luciferase activity (Figure 4H).

To clarify whether the EC-Foxp1-Cdkn1b pathway regulates EC proliferation and contributes to neointimal formation, we constructed RGD (Arg-Gly-Asp)-peptide magnetic nanoparticles to target deliver Cdkn1b-siRNA and rescue the EC-Foxp1 deletion-mediated impaired EC repair in *Foxp1^{ECKO}* mice. 65% decreased Cdkn1b expression following RGD (Arg-Gly-Asp)-peptide

Figure 4. Endothelial cell (EC)-Foxp1 (forkhead box P1) regulates cyclin dependent kinase inhibitor 1B (Cdkn1b) expression contributing to endothelial repair after injury denudation and neointimal formation.

A, EC-Foxp1 deletion mice exhibit significant less EC coverage of whole mount femoral artery by in situ Evans blue staining at 7 days after wire injury compared with wild-type littermate control mice, with representative images (left) and quantification (right) ($n=6$ for each group). **B** through **D**, Human umbilical vein endothelial cells (HUVECs) treated with lentiviral Foxp1-shRNA display decreased cell proliferation in comparison with HUVECs treated with lentiviral scramble-shRNA, shown by cell counting (B), 3-(4, 5-dimethylthiazol-2-yl)-2, 5-diphenyltetrazolium bromide assay (C) and Ki67 staining with quantification on the right (D) ($n=5$). Statistical values of cell counting and MMT are shown in Data S2. **E** and **F**, HUVECs treated with lentiviral Foxp1-shRNA display increased expression of Cdkn1b shown by real-time quantitative reverse transcription polymerase chain reaction (E) and Western blot (F) compared with HUVECs treated with lentiviral scramble-shRNA ($n=5$). **G**, Chromatin immunoprecipitation assay shows that Foxp1 binds to the mouse Cdkn1b promoter by quantitative polymerase chain reaction (down) with agarose gel (up) ($n=5$). **H**, The promoter region of Cdkn1b, -1.4 kb before Exon 1 has 3 Foxp1-binding sites (left) and luciferase assay shows that Foxp1 expression vector dose-dependent suppresses the luciferase reporter activity of this Cdkn1b promoter region (right) ($n=5$). **I**, The efficiency of decreased Cdkn1b expression following RGD (Arg-Gly-Asp)-peptide magnetic nanoparticle application was confirmed by real-time quantitative reverse transcription polymerase chain reaction in lung ECs ($n=8$). **J**, RGD (Arg-Gly-Asp)-nanoparticles target delivery of Cdkn1b-siRNA to endothelial cells (ECs) reverses the Foxp1 deletion-mediated decreased EC repair following wire injury, shown by in situ Evans blue staining of femoral artery ($n=8$). **K**, Decreased expression of Cdkn1b in HUVECs treated with Cdkn1b-siRNA is confirmed by real-time quantitative reverse transcription polymerase chain reaction and Western blot ($n=5$). **L** through **N**, Cdkn1b-siRNA knockdown HUVECs reverses the Foxp1 knockdown-mediated decrease of cell proliferation in comparison with HUVECs treated with scramble-siRNA, shown by cell counting (L), 3-(4, 5-dimethylthiazol-2-yl)-2, 5-diphenyltetrazolium bromide assay (M) and Ki67 staining with quantification on the right (N) ($n=5$). Statistical values of cell counting and MMT are shown in Data S2. Data are means \pm SEM. Cdkn1b indicates cyclin dependent kinase inhibitor 1B; Foxp1, forkhead box P1; HUVECs, human umbilical vein endothelial cells; IgG, immunoglobulin G; MMP9, matrix metalloproteinase-9; NC, negative control; OD, optical density; and WT, wild-type. * $P<0.05$, ** $P<0.01$. Scale bars: A, J=1 mm; D, N=100 μ m.



magnetic nanoparticle application was assessed by RT-qPCR in lung ECs ($P=0.009$) (Figure 4I). We found that in vivo EC-Cdkn1b knockdown significantly improved the repair of the EC denuded femoral artery from $64.6\pm 3.2\%$ to $78.9\pm 4.3\%$ by Evans blue staining ($P=0.024$). Furthermore, EC-Cdkn1b knockdown reversed the impaired EC repair of the EC denuded femoral artery in Foxp1^{ECKO} mutant mice from $51.4\pm 3.1\%$

to $70.3\pm 2.5\%$ ($P=0.002$) (Figure 4J), suggesting that the EC-Foxp1-Cdkn1b signal might regulate EC repair contributing to in vivo neointimal formation.

To further confirm these in vivo findings, we used siRNA to knockdown Cdkn1b and investigate the effects of Cdkn1b on EC-Foxp1 deletion-mediated decreased proliferation in in vitro cultured HUVECs. The efficiency of decreased Cdkn1b expression in HUVECs

was confirmed by RT-qPCR (88% reduction; $P=0.001$) and Western blot (Figure 4K). Cdkn1b-siRNA in HUVECs increased cell proliferation assessed by cell counting ($5.6\pm 0.4\times 10^4$ to $8.3\pm 0.5\times 10^4$ at 24 hours; $P=0.010$, $8.6\pm 0.6\times 10^4$ to $12.5\pm 0.7\times 10^4$ at 48 hours; $P=0.016$), MTT assay (1.6 ± 0.07 to 2.2 ± 0.1 at 24 hours; $P=0.030$, 2.4 ± 0.1 to 3.5 ± 0.2 , $P=0.007$ at 48 hours), and Ki67 staining assay ($22.7\pm 1.9\%$ to $30.2\pm 2.2\%$; $P=0.016$). We further found that Cdkn1b-siRNA normalized the EC-Foxp1 knockdown-mediated decreased cell proliferation compared with scramble siRNA by cell counting ($4.0\pm 0.3\times 10^4$ to $6.6\pm 0.3\times 10^4$ at 24 hours; $P=0.002$, $5.9\pm 0.5\times 10^4$ to $9.4\pm 0.5\times 10^4$ at 48 hours; $P=0.005$), MTT assay (1.1 ± 0.05 to 1.9 ± 0.1 at 24 hours; $P=0.003$, 1.7 ± 0.1 to 2.6 ± 0.2 at 48 hours; $P=0.018$), and Ki67 staining assay ($13.5\pm 1.1\%$ to $24.4\pm 1.9\%$; $P=0.005$); (Figure 4L and 4N), thus providing evidence that the EC-Foxp1-Cdkn1b pathway might regulate injury denuded EC repair through cell proliferation and control in vivo neointimal formation.

EC-Foxp1 Gain-of-Function Attenuates Wire Injury Induced Neointimal Formation Through Decreased VSMC Proliferation and Migration and Improved Endothelial Repair

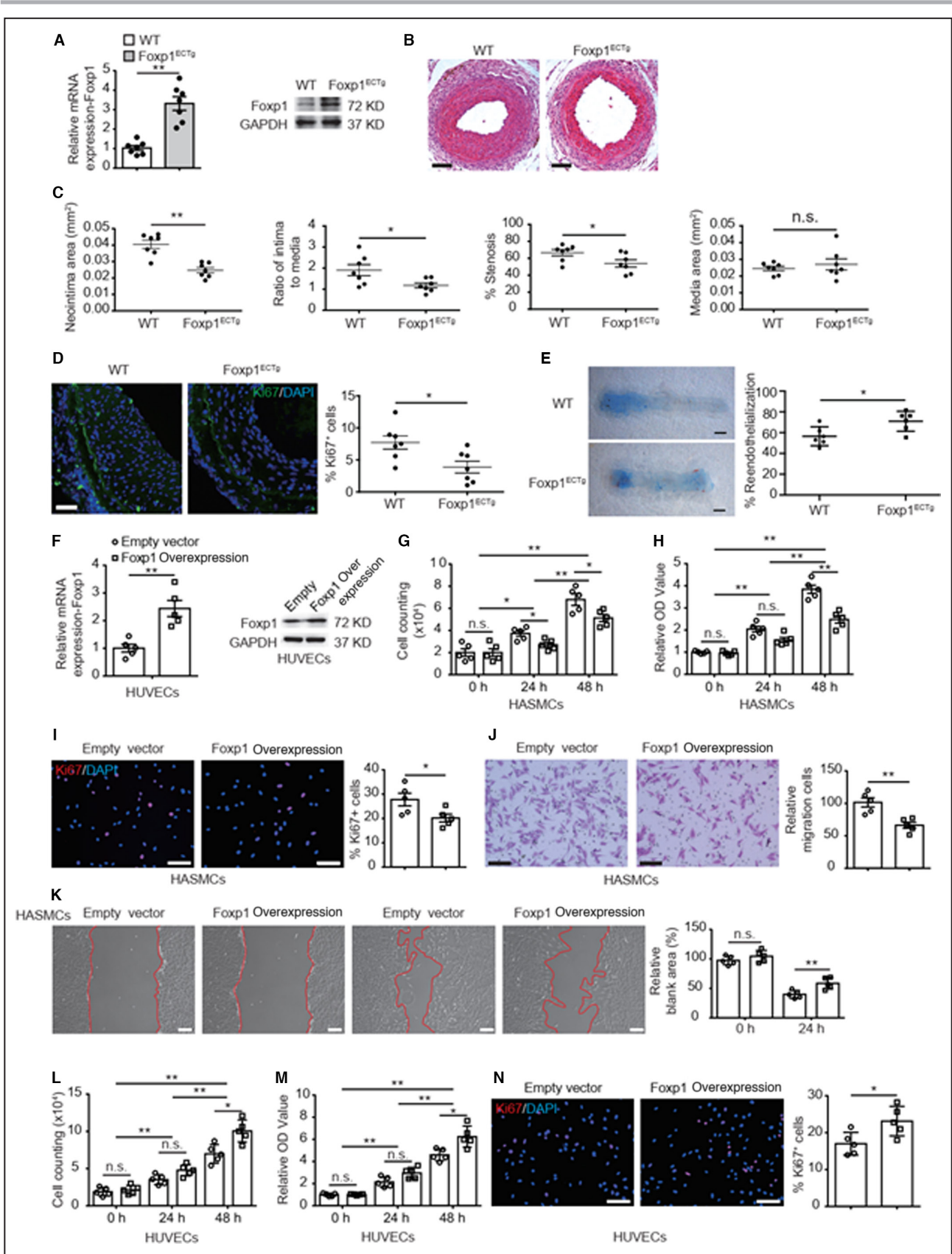
Contrary to EC-Foxp1 loss-of-function mice, EC-Foxp1 gain-of-function (*Foxp1^{ECTg}*) mice which had elevated Foxp1 expression in ECs (2.3-fold increase by RT-qPCR; $P=0.001$) (Figure 5A), displayed decreased neointimal area from $0.04\pm 0.002\ \mu\text{m}^2$ to $0.02\pm 0.002\ \mu\text{m}^2$ ($P=0.001$), intima-to-media ratio from 1.9 ± 0.3 to 1.1 ± 0.1 ($P=0.012$) and percentage of stenosis from $66.7\pm 3.6\%$ to $48.6\pm 3.9\%$ ($P=0.005$), with no change

in media area from $0.02\pm 0.001\ \mu\text{m}^2$ to $0.02\pm 0.003\ \mu\text{m}^2$ ($P>0.05$) (Figure 5B and 5C). VSMC proliferation in the neointima of *Foxp1^{ECTg}* mice was decreased from $7.7\pm 1.0\%$ to $3.9\pm 0.9\%$ assessed by Ki67 antibody immunostaining compared with the littermate WT control mice ($P=0.017$) (Figure 5D), and EC repair in *Foxp1^{ECTg}* mice was improved evaluated by Evans blue staining at day 7 after femoral artery injury (WT $56.5\pm 3.7\%$ versus *Foxp1^{ECTg}* $70.5\pm 4.1\%$; $P=0.030$) (Figure 5E). We found reduced MMP9 (71.8% reduction; $P=0.004$) and Cdkn1b (53.5% reduction; $P=0.016$) expression in ECs of *Foxp1^{ECTg}* mice compared with littermate WT control mice (Figure S5A). Recombinant MMP9 protein (rMMP9) significantly reversed the reduction of neointimal hyperplasia in *Foxp1^{ECTg}* mice assessed by intima-to-media ratio (PBS 1.2 ± 0.2 versus rMMP9 2.3 ± 0.2 ; $P=0.003$), percent of stenosis (PBS $57.8\pm 2.0\%$ versus rMMP9 $80.3\pm 2.4\%$; $P=0.001$), and reduced Ki67-positive cells immunostaining (PBS $3.1\pm 0.6\%$ versus rMMP9 $11.6\pm 1.7\%$; $P=0.001$) in the wire injury femoral artery (Figure S5B and S5C).

We then overexpressed Foxp1 in HUVECs and investigated the effects of EC-Foxp1 gain-of-function on VSMC proliferation and migration. Foxp1 overexpression was confirmed by RT-qPCR (1.4-fold increase; $P=0.002$) and Western blot (Figure 5F), and Foxp1 overexpression in HUVEC significantly decreased the cell proliferation of human aortic smooth muscle cells as shown by cell counting (empty $3.7\pm 0.2\times 10^4$ versus Foxp1 overexpression $2.7\pm 0.2\times 10^4$ at 24 hours; $P=0.046$, empty $6.8\pm 0.4\times 10^4$ versus Foxp1 OE $5.1\pm 0.3\times 10^4$ at 48 hours; $P=0.043$), MTT assay (empty 3.8 ± 0.2 versus Foxp1 overexpression 2.5 ± 0.2 ; $P=0.002$), and Ki67 staining (empty $27.8\pm 2.6\%$ versus $20.2\pm 1.6\%$; $P=0.038$) (Figure 5G through Figure 5I). The

Figure 5. Endothelial cell (EC)-Foxp1 (forkhead box P1) gain-of-function attenuates vascular neointimal formation through facilitation of EC repair and reduction of vascular smooth muscle cell proliferation and migration after wire injury.

A, EC-Foxp1 gain-of-function mice (*Foxp1^{ECTg}*) exhibit a significant increase of Foxp1 expression in vascular ECs compared with wild-type mice by real-time quantitative reverse transcription polymerase chain reaction (left) and Western blot (right) ($n=7$). **B** and **C**, *Foxp1^{ECTg}* mutant mice exhibit decreased neointimal formation at 28 days after femoral artery wire injury compared with wild-type littermates, with representative images (B) and quantification of neointima area, intima to media ratio, percentage stenosis and media area (C) ($n=7$ for each group). **D**, *Foxp1^{ECTg}* mutant mice exhibit significantly decreased cell proliferation in neointima at 28 d after femoral artery wire injury, with representative images (left) and quantification data (right) ($n=7$ for each group). **E**, *Foxp1^{ECTg}* mutant mice exhibit a significant increase of EC coverage of femoral artery by in situ Evans blue staining at 7 days following wire injury compared with wild-type littermates, with representative images (left) and quantification (right) ($n=6$ for each group). **F**, Real-time quantitative reverse transcription polymerase chain reaction and Western blot confirm the significant increase of Foxp1 expression in human umbilical vein endothelial cells (HUVECs) treated with Foxp1 overexpression vector compared with empty control vector ($n=5$). **G** through **I**, Condition medium from Foxp1 overexpression HUVECs significantly inhibits human aortic smooth muscle cell proliferation compared with that from HUVECs of control vector, shown by cell counting (G), 3-(4, 5-dimethylthiazol-2-yl)-2, 5-diphenyltetrazolium bromide assay (H), and Ki67 staining with quantification of Ki67-positive cells on the right (I) ($n=5$). Statistical values of cell counting and MMT are shown in Data S2. **J** and **K**, Condition medium from Foxp1 overexpression HUVECs significantly inhibits human aortic smooth muscle cell migration compared with that from HUVECs of control vector, shown by transwell (J) and wound healing assay (K), with representative images (left) and quantification (right) ($n=5$). **L** through **N**, Foxp1 overexpression in HUVECs increases cell proliferation in comparison with that of control vector, shown by cell counting (L), 3-(4, 5-dimethylthiazol-2-yl)-2, 5-diphenyltetrazolium bromide assay (M) and Ki67 staining with quantification on the right (N) ($n=5$). Statistical values of cell counting and MMT are shown in Data S2. Data are means \pm SEM. Foxp1 indicates forkhead box P1; HASMCs, human aortic muscle cells; HUVECs, human umbilical vein endothelial cells; MMP9, matrix metalloproteinase-9; OD, optical density; and WT, wild-type. * $P<0.05$, ** $P<0.01$. Scale bars: B, D, I, J, K, N=100 μm ; E=1 mm.



condition medium of Foxp1 overexpressed HUVECs also significantly reduced the migration of human aortic smooth muscle cells shown by transwell chemotactic (empty 100.0 ± 7.1 versus Foxp1 overexpression 66.3 ± 4.6 ; $P=0.003$) and wound healing assay (empty 39.9 ± 2.9 versus Foxp1 overexpression 58.5 ± 4.2 ; $P=0.006$) (Figure 5J and 5K). Moreover, The HUVECs of Foxp1 overexpression exhibited increase of cell proliferation shown by cell counting (empty $7.0 \pm 0.6 \times 10^4$ versus Foxp1 overexpression $10.1 \pm 0.7 \times 10^4$; $P=0.029$), MTT assay (empty 4.6 ± 0.2 versus Foxp1 overexpression 6.2 ± 0.4 ; $P=0.042$), and Ki67 staining (empty $17.0 \pm 1.4\%$ versus Foxp1 overexpression 23.1 ± 1.8 ; $P=0.026$) (Figure 5L and Figure 5N) and increase of cell migration shown by wound healing (empty 56.9 ± 2.6 versus Foxp1 overexpression 29.7 ± 2.4 ; $P=0.001$) and transwell chemotactic assay (empty 100.0 ± 5.7 versus Foxp1 overexpression 204.7 ± 10.6 ; $P=0.001$) (Figure S6). EC-Cdkn1b overexpression reversed the EC-Foxp1 gain-of-function-mediated increase of EC proliferation compared with the control empty vector by cell counting (empty 3.6 ± 0.2 versus Cdkn1b overexpression 3.0 ± 0.1 at 24 hours; $P=0.039$, empty 8.4 ± 0.3 versus Cdkn1b overexpression 6.7 ± 0.3 at 48 hours; $P=0.007$) and MTT (empty 1.6 ± 0.07 versus Cdkn1b overexpression 1.3 ± 0.05 at 24 hours; $P=0.018$, empty 3.6 ± 0.15 versus Cdkn1b overexpression 2.2 ± 0.07 at 48 hours; $P=0.007$) (Figure S5D through S5F). These

data indicate that EC-Foxp1 overexpression restricts VSMC proliferation and migration and improves EC repair leading to the attenuation of neointimal hyperplasia in vivo via EC-Foxp1-MMP9/Cdkn1b signaling pathway.

Overall, our data reveal that EC-Foxp1 reduces MMP9 expression to restrict VSMCs proliferation and migration, as well as suppresses Cdkn1b expression to promote EC proliferation for improvement of EC repair, and that both work together resulted in the attenuation of the injury induced neointimal hyperplasia (Figure 6).

DISCUSSION

Vascular stent placement has become a common procedure in cardiovascular disease, which can dredge occluded vessels and restore blood flow. However, stent deployment causes injury of vascular endothelium followed by excess VSMC proliferation and migration contributing to neointimal hyperplasia and hence restenosis, which is still a clinical problem, although stent technology advances have incrementally improved the outcomes. Foxp1 was reported to be important in EC proliferation and migration,¹⁸ and our previous study demonstrated an important role of EC-Foxp1 in the regulation of cardiomyocyte proliferation,¹⁶ cardiac fibroblast proliferation, and myofibroblast

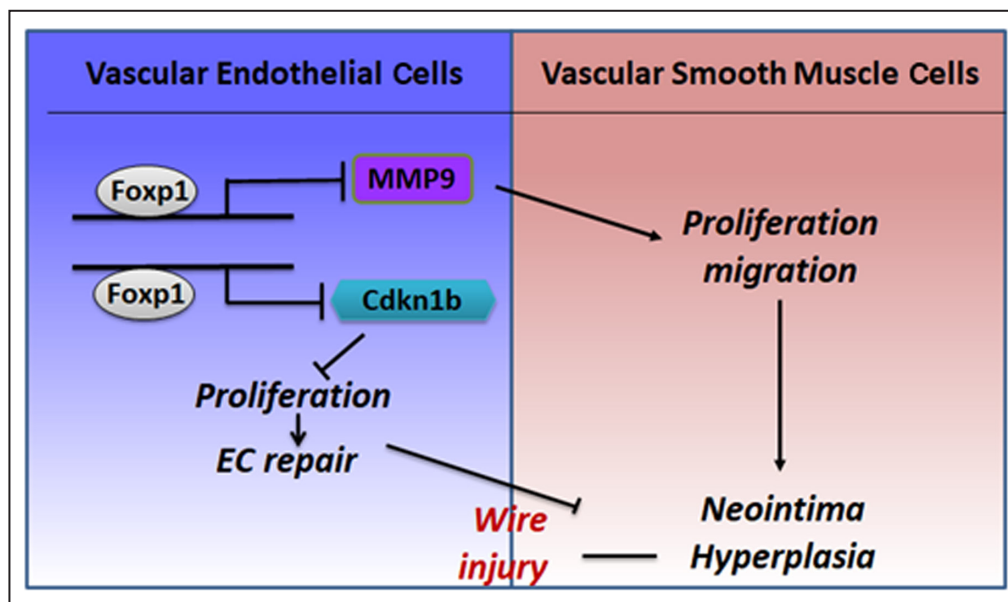


Figure 6. Working model of how endothelial cell-Foxp1 (forkhead box P1) regulates neointimal hyperplasia through matrix metalloproteinase-9/cyclin dependent kinase inhibitor 1B signal pathway following femoral artery injury.

Endothelial cell-Foxp1 paracrine reduces matrix metalloproteinase-9 expression to restrict vascular smooth muscle cells proliferation and migration and suppresses cyclin dependent kinase inhibitor 1B expression to promote endothelial cell proliferation for improvement of endothelial cell repair, and both work together leading to the attenuation of the injury induced neointimal hyperplasia. Cdkn1b indicates cyclin dependent kinase inhibitor 1B; EC, endothelial cells; Foxp1, forkhead box P1; MMP9, matrix metalloproteinase-9; and WT, wild-type.

transformation.¹⁷ The present study demonstrated that EC-Foxp1 regulates the MMP9/Cdkn1b signaling pathway to control VSMC proliferation/migration and reendothelialization, thus, we uncovered a novel role of EC-Foxp1 in neointimal hyperplasia responsible for restenosis.

During the process of neointimal hyperplasia, VSMCs can transform from the static contractile state to the proliferative synthetic state in the response to pathological stimuli. Loss of endothelium or activated dysfunctional ECs induced excessive proliferation and migration of synthetic SMCs until endothelium is functionally recovered.^{4–8}

MMP9, one member of the MMP family, participates in the degradation of the ECM in the physiological and pathophysiological processes involving tissue remodeling associated with cardiovascular diseases.^{31–34} MMP9 is secreted by neutrophils, macrophages, and fibroblasts.^{31,32} MMP9 is also detected in vascular ECs and VSMC and it is important for early-stage arterial remodeling and causes a rise in pressure through altered vessel distensibility responsible for hypertension.³³ The 3 key target regulation genes of myocardin-related transcription factor-A/serum response factor, including vinculin, MMP-9, and integrin β 1, were reported to regulate VSMC migration and are crucial for pathological vascular remodeling in mice.³⁴ Also, MMP9 was activated after arterial injury³⁵ and during preparation of vein grafts³⁶ and it is essential for the migration of smooth muscle cells into the intima contributing to injury induced neointimal formation.³⁷ MMP9 was involved in proangiogenic EC function and endothelial cell mediated medial disruption during the progression of abdominal aortic aneurysm.³⁸ However, it was still unknown about the transcriptional regulation of MMP9 expression in ECs and the roles of EC-MMP9 in neointimal formation. Our data indicate that EC-Foxp1 directly regulates MMP9 expression and increase of MMP9 and neointimal formation caused by loss-of Foxp1 in ECs could be rescued by local delivery of lentiviral MMP9 shRNA to the injured artery, therefore providing in vivo evidence that EC-Foxp1-MMP9 pathway may be therapeutic targets for injury-induced neointimal formation.

A healthy EC layer is the most important factor in maintaining vascular homeostasis. PCI stent deployment causes vascular injury and damaged ECs are repaired by locally derived ECs.¹² Delayed and impaired endothelial recovery are involved in late stent restenosis and thrombosis.^{13,39} The biological factors and the cellular and molecular mechanisms that govern the reendothelialization process are not clear. Loss of endothelial protein tyrosine phosphatase-1B, a negative regulator of receptor tyrosine kinase signaling for cell proliferation and senescence, impaired reendothelialization and the failure to induce smooth muscle cell

quiescence and resulted in neointimal hyperplasia.⁴⁰ A recent study found that activation of the transcription factor FOXO1 (forkhead box O1) in ECs limited cell cycle progression, metabolic activity, and vascular expansion.⁴¹ Foxp1 was essential in the regulation of EC proliferation and migration.¹⁸ A previous study demonstrated that EC-MMP9 promoted angiogenesis through activating PAR1 in apoE^{-/-} mice,⁴² however, we did not find significant change of EC proliferation and migration in the baseline unstimulated condition (data not shown). Possibly MMPs might exert different effects on baseline or prestenotic condition in comparison with the proinflammatory condition in apoE^{-/-} mice. Moreover, we found MMP9 knockdown did not change the decreased EC proliferation upon EC-Foxp1 deletion (data not shown). Therefore, we further explored the mechanisms, and we found regulation of EC-Foxp1 for Cdkn1b to control endothelial repair and hence neointimal formation. Delivery of Cdkn1b-siRNA using RGD (Arg-Gly-Asp)-peptide magnetic nanoparticle to ECs reversed the EC-Foxp1 deletion-mediated impaired EC repair and attenuated the neointimal formation, thus providing in vivo evidence of EC-Foxp1 regulation of Cdkn1b controlling reendothelialization of endothelial injury and further influencing neointimal hyperplasia.

Taken together, these data using both EC-Foxp1 loss- and gain-of-function mice demonstrate that EC-Foxp1 regulates injury induced neointimal formation by paracrine modulation of MMP9 for VSMC proliferation and migration and cell autonomous modulation of Cdkn1b of reendothelialization controlling neointimal formation. The EC target delivery of MMP9/Cdkn1b might provide future novel therapeutic interventions for restenosis.

ARTICLE INFORMATION

Received April 6, 2022; accepted June 20, 2022.

Affiliations

Key Laboratory of Arrhythmias of the Ministry of Education of China, Research Center for Translational Medicine (X.C., J.X., W.B., H.L., W.W., J.L., L.Z., H.F., Z.L., Y.Z., J.L., T.Z.), and Department of Cardiology (J.P., Q.Z., L.L.), Shanghai East Hospital, Tongji University School of Medicine, Shanghai, China; Faculty of Medicine, Macau University of Science and Technology, Macau, China (B.T.); Division of Cardiology, Department of Internal Medicine, Wan Fang Hospital, Taipei Medical University, Taipei, Taiwan (P.C.); Department of Physiology and Pathophysiology School of Basic Medical Sciences (C.R., T.Z.); and Shanghai Jinshan Eye Disease Prevention and Treatment Institute, Shanghai Jinshan Nuclear and Chemical Injury Emergency Treatment Center, Jinshan Hospital (T.Z.), Fudan University, Shanghai, China; and Department of Cell and Developmental Biology (R.W., E.E.M.), Department of Medicine (E.E.M.), Penn Cardiovascular Institute (E.E.M.), and Penn Institute for Regenerative Medicine (E.E.M.), University of Pennsylvania, Philadelphia, Pennsylvania (E.M.).

Sources of Funding

This study was supported by the funds from the National Natural Science Foundation of China (Grant No. 82070456, 81800253, 81970233, 81770259, 81970234, 81970232, 81903174, 81770094, 81870202, 81570237, 81870197), Shanghai Rising-Star Program (Grant no. 21QA1401400,

20QA1408100), Shanghai Science and Technology innovation Action Plan (Grant no. 19JC1414500), Health System Academic Leader Training Plan of Pudong District Shanghai (Grant no. PWRd2018-06), Peak Disciplines (Type IV) of Institutions of Higher Learning in Shanghai.

Disclosures

None.

Supplemental Material

Data S1–S2

Tables S1–S4

Figures S1–S6

References 43–50

REFERENCES

- Serruys PW, Ono M, Garg S, Hara H, Kawashima H, Pompilio G, Andreini D, Holmes DR Jr, Onuma Y, King Iii SB. Percutaneous coronary revascularization: JACC historical breakthroughs in perspective. *J Am Coll Cardiol*. 2021;78:384–407. doi: 10.1016/j.jacc.2021.05.024
- Chacko L, Howard JP, Rajkumar C, Nowbar AN, Kane C, Mahdi D, Foley M, Shun-Shin M, Cole G, Sen S, et al. Effects of percutaneous coronary intervention on death and myocardial infarction stratified by stable and unstable coronary artery disease: a meta-analysis of randomized controlled trials. *Circ Cardiovasc Qual Outcomes*. 2020;13:e006363. doi: 10.1161/CIRCOUTCOMES.119.006363
- Yang X, Yang Y, Guo J, Meng Y, Li M, Yang P, Liu X, Aung LHH, Yu T, Li Y. Targeting the epigenome in in-stent restenosis: from mechanisms to therapy. *Mol Ther Nucleic Acids*. 2021;23:1136–1160. doi: 10.1016/j.omtn.2021.01.024
- Otsuka F, Finn AV, Yazdani SK, Nakano M, Kolodgie FD, Virmani R. The importance of the endothelium in atherothrombosis and coronary stenting. *Nat Rev Cardiol*. 2012;9:439–453. doi: 10.1038/nrcardio.2012.64
- Marx SO, Totary-Jain H, Marks AR. Vascular smooth muscle cell proliferation in restenosis. *Circ Cardiovasc Interv*. 2011;4:104–111. doi: 10.1161/CIRCINTERVENTIONS.110.957332
- Owens GK, Kumar MS, Wamhoff BR. Molecular regulation of vascular smooth muscle cell differentiation in development and disease. *Physiol Rev*. 2004;84:767–801. doi: 10.1152/physrev.00041.2003
- Cornelissen A, Vogt FJ. The effects of stenting on coronary endothelium from a molecular biological view: time for improvement? *J Cell Mol Med*. 2019;23:39–46. doi: 10.1111/jcmm.13936
- van Beusekom HM, Whelan DM, Hofma SH, Krabbendam SC, van Hinsbergh VW, Verdouw PD, van der Giessen WJ. Long-term endothelial dysfunction is more pronounced after stenting than after balloon angioplasty in porcine coronary arteries. *J Am Coll Cardiol*. 1998;32:1109–1117. doi: 10.1016/s0735-1097(98)00348-9
- Wang J, Jin X, Huang Y, Ran X, Luo D, Yang D, Jia D, Zhang K, Tong J, Deng X, et al. Endovascular stent-induced alterations in host artery mechanical environments and their roles in stent restenosis and late thrombosis. *Regen Biomater*. 2018;5:177–187. doi: 10.1093/rb/rby006
- Zhuang T, Liu J, Chen X, Pi J, Kuang Y, Wang Y, Tomlinson B, Chan P, Zhang Q, Li Y, et al. Cell-specific effects of GATA (GATA zinc finger transcription factor family)-6 in vascular smooth muscle and endothelial cells on vascular injury neointimal formation. *Arterioscler Thromb Vasc Biol*. 2019;39:888–901. doi: 10.1161/ATVBAHA.118.312263
- Wang X, Fang F, Ni Y, Yu H, Ma J, Deng L, Li C, Shen Y, Liu X. The combined contribution of vascular endothelial cell migration and adhesion to stent re-endothelialization. *Front Cell Dev Biol*. 2021;9:641382. doi: 10.3389/fcell.2021.641382
- Van der Heiden K, Gijsen FJ, Narracott A, Hsiao S, Halliday I, Gunn J, Wentzel JJ, Evans PC. The effects of stenting on shear stress: relevance to endothelial injury and repair. *Cardiovasc Res*. 2013;99:269–275. doi: 10.1093/cvr/cvt090
- Hutter R, Carrick FE, Valdiviezo C, Wolinsky C, Rudge JS, Wiegand SJ, Fuster V, Badimon JJ, Sauter BV. Vascular endothelial growth factor regulates reendothelialization and neointima formation in a mouse model of arterial injury. *Circulation*. 2004;110:2430–2435. doi: 10.1161/01.CIR.0000145120.37891.8A
- Li S, Weidenfeld J, Morrisey EE. Transcriptional and DNA binding activity of the Foxp1/2/4 family is modulated by heterotypic and homotypic protein interactions. *Mol Cell Biol*. 2004;24:809–822. doi: 10.1128/MCB.24.2.809-822.2004
- Shu W, Yang H, Zhang L, Lu MM, Morrisey EE. Characterization of a new subfamily of winged-helix/forkhead (fox) genes that are expressed in the lung and act as transcriptional repressors. *J Biol Chem*. 2001;276:27488–27497. doi: 10.1074/jbc.M100636200
- Zhang Y, Li S, Yuan L, Tian Y, Weidenfeld J, Yang J, Liu F, Chokas AL, Morrisey EE. Foxp1 coordinates cardiomyocyte proliferation through both cell-autonomous and nonautonomous mechanisms. *Genes Dev*. 2010;24:1746–1757. doi: 10.1101/gad.1929210
- Liu J, Zhuang T, Pi J, Chen X, Zhang Q, Li Y, Wang H, Shen Y, Tomlinson B, Chan P, et al. Endothelial Forkhead box transcription factor P1 regulates pathological cardiac remodeling through transforming growth factor-beta1-Endothelin-1 signal pathway. *Circulation*. 2019;140:665–680. doi: 10.1161/CIRCULATIONAHA.119.039767
- Grundmann S, Lindmayer C, Hans FP, Hoefer I, Helbing T, Pasterkamp G, Bode C, de Kleijn D, Moser M. FoxP1 stimulates angiogenesis by repressing the inhibitory guidance protein semaphorin 5B in endothelial cells. *PLoS One*. 2013;8:e70873. doi: 10.1371/journal.pone.0070873
- Wang H, Geng J, Wen X, Bi E, Kossenkov AV, Wolf AI, Tas J, Choi YS, Takata H, Day TJ, et al. The transcription factor Foxp1 is a critical negative regulator of the differentiation of follicular helper T cells. *Nat Immunol*. 2014;15:667–675. doi: 10.1038/ni.2890
- Wang Y, Nakayama M, Pitulescu ME, Schmidt TS, Bochenek ML, Sakakibara A, Adams S, Davy A, Deutsch U, Luthi U, et al. Ephrin-B2 controls VEGF-induced angiogenesis and lymphangiogenesis. *Nature*. 2010;465:483–486. doi: 10.1038/nature09002
- Zhuang T, Liu J, Chen X, Zhang L, Pi J, Sun H, Li L, Bauer R, Wang H, Yu Z, et al. Endothelial Foxp1 suppresses atherosclerosis via modulation of Nlrp3 inflammasome activation. *Circ Res*. 2019;125:590–605. doi: 10.1161/CIRCRESAHA.118.314402
- Li H, Wang Y, Liu J, Chen X, Duan Y, Wang X, Shen Y, Kuang Y, Zhuang T, Tomlinson B, et al. Endothelial Klf2-Foxp1-TGFbeta signal mediates the inhibitory effects of simvastatin on maladaptive cardiac remodeling. *Theranostics*. 2021;11:1609–1625. doi: 10.7150/thno.48153
- Bot PT, Grundmann S, Goumans MJ, de Kleijn D, Moll F, de Boer O, van der Wal AC, van Soest A, de Vries JP, van Royen N, et al. Forkhead box protein P1 as a downstream target of transforming growth factor-beta induces collagen synthesis and correlates with a more stable plaque phenotype. *Atherosclerosis*. 2011;218:33–43. doi: 10.1016/j.atherosclerosis.2011.05.017
- Chappell J, Harman JL, Narasimhan VM, Yu H, Foote K, Simons BD, Bennett MR, Jorgensen HF. Extensive proliferation of a subset of differentiated, yet plastic, medial vascular smooth muscle cells contributes to neointimal formation in mouse injury and atherosclerosis models. *Circ Res*. 2016;119:1313–1323. doi: 10.1161/CIRCRESAHA.116.309799
- Mason DP, Kenagy RD, Hasenstab D, Bowen-Pope DF, Seifert RA, Coats S, Hawkins SM, Clowes AW. Matrix metalloproteinase-9 overexpression enhances vascular smooth muscle cell migration and alters remodeling in the injured rat carotid artery. *Circ Res*. 1999;85:1179–1185. doi: 10.1161/01.res.85.12.1179
- Johnson JL, Dwivedi A, Somerville M, George SJ, Newby AC. Matrix metalloproteinase (MMP)-3 activates MMP-9 mediated vascular smooth muscle cell migration and neointima formation in mice. *Arterioscler Thromb Vasc Biol*. 2011;31:e35–e44. doi: 10.1161/ATVBAHA.111.225623
- Gliesche DG, Hussner J, Witzigmann D, Porta F, Glatter T, Schmidt A, Huwylar J, Meyer Zu Schwabedissen HE. Secreted matrix Metalloproteinase-9 of proliferating smooth muscle cells as a trigger for drug release from stent surface polymers in coronary arteries. *Mol Pharm*. 2016;13:2290–2300. doi: 10.1021/acs.molpharmaceut.6b00033
- Testamariam B. Endothelial repair and regeneration following intimal injury. *J Cardiovasc Transl Res*. 2016;9:91–101. doi: 10.1007/s12265-016-9677-1
- Jian D, Wang W, Zhou X, Jia Z, Wang J, Yang M, Zhao W, Jiang Z, Hu X, Zhu J. Interferon-induced protein 35 inhibits endothelial cell proliferation, migration and re-endothelialization of injured arteries by inhibiting the nuclear factor-kappa B pathway. *Acta Physiol*. 2018;223:e13037. doi: 10.1111/apha.13037
- Lam EW, Brosens JJ, Gomes AR, Koo CY. Forkhead box proteins: tuning forks for transcriptional harmony. *Nat Rev Cancer*. 2013;13:482–495. doi: 10.1038/nrc3539
- Yabluchanskiy A, Ma Y, Iyer RP, Hall ME, Lindsey ML. Matrix metalloproteinase-9: many shades of function in cardiovascular disease. *Physiology*. 2013;28:391–403. doi: 10.1152/physiol.00029.2013

32. Siefert SA, Sarkar R. Matrix metalloproteinases in vascular physiology and disease. *Vascular*. 2012;20:210–216. doi: [10.1258/vasc.2011.201202](https://doi.org/10.1258/vasc.2011.201202)
33. Lehoux S, Lemarie CA, Esposito B, Lijnen HR, Tedgui A. Pressure-induced matrix metalloproteinase-9 contributes to early hypertensive remodeling. *Circulation*. 2004;109:1041–1047. doi: [10.1161/01.CIR.0000115521.95662.7A](https://doi.org/10.1161/01.CIR.0000115521.95662.7A)
34. Minami T, Kuwahara K, Nakagawa Y, Takaoka M, Kinoshita H, Nakao K, Kuwabara Y, Yamada Y, Yamada C, Shibata J, et al. Reciprocal expression of MRTF-A and myocardin is crucial for pathological vascular remodeling in mice. *EMBO J*. 2012;31:4428–4440. doi: [10.1038/emboj.2012.296](https://doi.org/10.1038/emboj.2012.296)
35. Zempo N, Kenagy RD, Au YP, Bendeck M, Clowes MM, Reidy MA, Clowes AW. Matrix metalloproteinases of vascular wall cells are increased in balloon-injured rat carotid artery. *J Vasc Surg*. 1994;20:209–217. doi: [10.1016/0741-5214\(94\)90008-6](https://doi.org/10.1016/0741-5214(94)90008-6)
36. George SJ, Zaltsman AB, Newby AC. Surgical preparative injury and neointima formation increase MMP-9 expression and MMP-2 activation in human saphenous vein. *Cardiovasc Res*. 1997;33:447–459. doi: [10.1016/s0008-6363\(96\)00211-8](https://doi.org/10.1016/s0008-6363(96)00211-8)
37. Cho A, Reidy MA. Matrix metalloproteinase-9 is necessary for the regulation of smooth muscle cell replication and migration after arterial injury. *Circ Res*. 2002;91:845–851. doi: [10.1161/01.res.0000040420.17366.2e](https://doi.org/10.1161/01.res.0000040420.17366.2e)
38. Ramella M, Boccafoschi F, Bellofatto K, Follenzi A, Fusaro L, Boldorini R, Casella F, Porta C, Settembrini P, Cannas M. Endothelial MMP-9 drives the inflammatory response in abdominal aortic aneurysm (AAA). *Am J Transl Res*. 2017;9:5485–5495.
39. Finn AV, Joner M, Nakazawa G, Kolodgie F, Newell J, John MC, Gold HK, Virmani R. Pathological correlates of late drug-eluting stent thrombosis: strut coverage as a marker of endothelialization. *Circulation*. 2007;115:2435–2441. doi: [10.1161/CIRCULATIONAHA.107.693739](https://doi.org/10.1161/CIRCULATIONAHA.107.693739)
40. Jager M, Hubert A, Gogiraju R, Bochenek ML, Munzel T, Schafer K. Inducible knockdown of endothelial protein tyrosine phosphatase-1B promotes neointima formation in obese mice by enhancing endothelial senescence. *Antioxid Redox Signal*. 2019;30:927–944. doi: [10.1089/ars.2017.7169](https://doi.org/10.1089/ars.2017.7169)
41. Andrade J, Shi C, Costa ASH, Choi J, Kim J, Doddaballapur A, Sugino T, Ong YT, Castro M, Zimmermann B, et al. Control of endothelial quiescence by FOXO-regulated metabolites. *Nat Cell Biol*. 2021;23:413–423. doi: [10.1038/s41556-021-00637-6](https://doi.org/10.1038/s41556-021-00637-6)
42. Florence JM, Krupa A, Booshehri LM, Allen TC, Kurdowska AK. Metalloproteinase-9 contributes to endothelial dysfunction in atherosclerosis via protease activated receptor-1. *PLoS One*. 2017;12:e0171427. doi: [10.1371/journal.pone.0171427](https://doi.org/10.1371/journal.pone.0171427)
43. Wang M, Ihida-Stansbury K, Kothapalli D, Tamby MC, Yu Z, Chen L, Grant G, Cheng Y, Lawson JA, Assoian RK, et al. Microsomal prostaglandin e2 synthase-1 modulates the response to vascular injury. *Circulation*. 2011;123:631–639. doi: [10.1161/CIRCULATIONAHA.110.973685](https://doi.org/10.1161/CIRCULATIONAHA.110.973685)
44. Konishi H, Sydow K, Cooke JP. Dimethylarginine dimethylaminohydrolyase promotes endothelial repair after vascular injury. *J Am Coll Cardiol*. 2007;49:1099–1105. doi: [10.1016/j.jacc.2006.10.068](https://doi.org/10.1016/j.jacc.2006.10.068)
45. Pi J, Tao T, Zhuang T, Sun H, Chen X, Liu J, Cheng Y, Yu Z, Zhu HH, Gao WQ, et al. A MicroRNA302-367-Erk1/2-Klf2-S1pr1 pathway prevents tumor growth via restricting angiogenesis and improving vascular stability. *Circ Res*. 2017;120:85–98. doi: [10.1161/CIRCRESAHA.116.309757](https://doi.org/10.1161/CIRCRESAHA.116.309757)
46. Akash MS, Rehman K, Li N, Gao JQ, Sun H, Chen S. Sustained delivery of IL-1Ra from pluronic F127-based thermosensitive gel prolongs its therapeutic potentials. *Pharm Res*. 2012;29:3475–3485. doi: [10.1007/s11095-012-0843-0](https://doi.org/10.1007/s11095-012-0843-0)
47. Lu MM, Li S, Yang H, Morrisey EE. Foxp4: a novel member of the Foxp subfamily of winged-helix genes co-expressed with Foxp1 and Foxp2 in pulmonary and gut tissues. *Gene Expr Patterns*. 2002;2:223–228. doi: [10.1016/s1567-133x\(02\)00058-3](https://doi.org/10.1016/s1567-133x(02)00058-3)
48. Banham AH, Beasley N, Campo E, Fernandez PL, Fidler C, Gatter K, Jones M, Mason DY, Prime JE, Trougouboff P, et al. The FOXP1 winged helix transcription factor is a novel candidate tumor suppressor gene on chromosome 3p. *Cancer Res*. 2001;61:8820–8829.
49. Lu MM, Li S, Yang H, Morrisey EE. Foxp4: a novel member of the Foxp subfamily of winged-helix genes co-expressed with Foxp1 and Foxp2 in pulmonary and gut tissues. *Mech Dev*. 2002;119:S197–S202. doi: [10.1016/s0925-4773\(03\)00116-3](https://doi.org/10.1016/s0925-4773(03)00116-3)
50. Tian Y, Zhang Y, Hurd L, Hannehalli S, Liu F, Lu MM, Morrisey EE. Regulation of lung endoderm progenitor cell behavior by miR302/367. *Development*. 2011;138:1235–1245. doi: [10.1242/dev.061762](https://doi.org/10.1242/dev.061762)

SUPPLEMENTAL MATERIAL

Data S1. Supplemental Methods

Animals

A conditional Foxp1 loss-of-function (*Foxp1^{fllox/fllox}*)¹⁶ or gain-of-function (*Foxp1^{Tg/Tg}*)¹⁹ mouse line was mated with endothelial specific promoter (Cdh5)-driven Cre recombinase line²⁰ to generate *Foxp1^{ECKO}* or *Foxp1^{ECTg}* mice for endothelial cell (EC)-specific deletion or overexpression of Foxp1 on C57BL/6 background.

Mouse Neointimal Hyperplasia Model and Quantification of Neointimal Formation

Murine femoral artery wire injury model was established in 8 to 10-week-old mice as described previously⁴³. Briefly, *Foxp1^{ECKO}* or *Foxp1^{ECTg}* mutant and wild-type littermate mice were performed left femoral artery injury using a flexible angioplasty wire (0.35-mm diameter; Cook Inc, Bloomington, IN) under 100 mg/kg Ketamine-HCl and 10 mg/kg xylazine HCl anesthesia and aseptic conditions. The mice were euthanized 28-day postsurgery and wire-injured femoral arteries were harvested, fixed with 4% paraformaldehyde, embedded in paraffin wax, and sectioned at 8 μ m intervals for histology analysis.

The cross-sections of the injured arteries were obtained at 500 μ m to 1500 μ m distant from the ligation at 100 μ m intervals. Sections were stained with hematoxylin and eosin (Servicebio, China) stain kit and the images were acquired with Leica DM750 microscope. Lumen circumference, the internal elastic lamina circumference, the circumference of the external elastic lamina were measured and then quantified using software Image J (Media Cybernetics, Bethesda, MD) as previously⁴. Measurements were performed with the observer blinded to experimental group.

Quantification of EC recovery following wire femoral artery injury

Endothelial repair was observed with Evans blue infiltration assay 7 days following femoral artery wire injury. Evans blue assay was performed as described previously⁴⁴. The injured femoral arteries were obtained 10 minutes after 50 μ l of 5% Evans blue injection via tail vein and opened longitudinally and the area of denudation stained by Evans blue was quantified under light microscopy with software Image J (n=6 for each group). Endothelial repair was calculated as ratio of the un-stained area to the total area.

RGD-Peptide magnetic nanoparticle delivery of Cdkn1b-siRNA to endothelial cells

Delivery of Cdkn1b-siRNA by RGD (Arg-Gly-Asp)-peptide magnetic nanoparticles to ECs was performed as previously⁴⁵. In brief, mouse Cdkn1b-siRNA (Table S2) or scramble-siRNA control was synthesized and formulated with RGD-peptide containing core Fe₃O₄ magnetic nanoparticles at the ratio of 10 μ g siRNA:50 μ g nanoparticles in total 100 μ l normal saline at room temperature for 1 hour. The RGD-peptide magnetic nanoparticles containing Cdkn1b-siRNA at the dose of 2 mg/kg were administrated by tail vein injection with a magnet on top of the injured legs following wire injury every four days.

Delivery of MMP9 *in vivo* to wire-injured femoral arteries

Briefly, 0.5 μ g recombinant human MMP9 (Novoprotein C171) dissolved in 100 μ l 30% pluronic gel was administrated perivascularly to the wire-injured femoral artery as described previously⁴⁶. The femoral arteries were harvested 28 days post-surgery for histological analysis.

Histology

The arteries sections were heat retrieved in sodium citrate buffer (10 mM, pH 6.0) for 20 minutes in 100°C water bath to perform antigen retrieval. The slices were permeabilized and blocked in PBS-T (0.02% triton X-100) with 1% goat serum for 1 hr. Immunostaining was performed using the following antibodies diluted in PBS-T at 4°C over-night: Rabbit anti-Foxp1⁴⁷, Rabbit anti-Ki67 (Abcam, ab16667), Rabbit anti-MMP9 (Proteintech, 10375-2-AP). After washing with PBS, sections were incubated with secondary antibodies (488 nm-conjugated

anti-rabbit secondary antibody) diluted in PBS-T for 1 hour at room temperature. Following wash with PBS for three times, slides were mounted with vectashield mounting medium containing DAPI (Vector Laboratories, Burlingame, CA, USA) and imaged using fluorescent microscope.

Cell culture and siRNA infection

Human umbilical vein endothelial cells (HUVECs, ATCC®PCS-100-010™) were cultured in EC growth medium 2 (EGM, Promocell C22010). Human aortic SMCs (HASMC) were obtained commercially (ATCC PCS-100-012) and maintained in Smooth Muscle Growth Medium (ATCC PCS-100-042) as manufacturer protocol. Cdkn1b siRNA was transfected to HUVECs with lipo2000 and the efficiency was assessed by RT-qPCR and western blot. The sequences of siRNA were listed in Table S2.

Subclone

The mouse and human full-length open reading frames of Foxp1 and Cdkn1b was constructed and subcloned into expressing vector as previously described⁴⁸. ShRNA of Foxp1 and MMP9 was inserted into pLKD vector. The sequences of gene-shRNA were listed in Table S2.

Cell proliferation assay

Cell proliferation assays includes cell counting, MTT assay and Ki67 staining assay. The cells were cultured in normal culture medium or endothelial cells condition medium during the process of cell proliferation assays. In cell counting assay, cells were seeded at an initial density of 2×10^4 per well in a 12-well plate and harvested and counted the cells at the designated time-points. In MTT assay, cells were seeded at 5×10^3 cells per well in a flat-bottom 96-well cell culture plate in culture medium or EC condition medium, 10 μ l of MTT (5 mg/ml) solution (Sigma) were added to each well at the designated time-points. Cell growth was determined by measuring the absorbance at 570 nm.

For Ki67 staining assay, serum-free starved cells were grown for 12 hours and stained with Ki67 antibody overnight at 4°C. After incubation with Alexa Fluor-conjugated secondary antibodies (1:1000; Invitrogen, Carlsbad, CA), the samples were mounted with vectashield mounting medium containing DAPI (Vector Laboratories, Burlingame, CA, USA) and were visualized using an inverted fluorescent microscope (Carl Zeiss, Oberkochen, Germany). Cell growth was determined by counting Ki67 positive cells in total cells.

Cell Migration assay

Migration assays were performed using scratch wound healing and transwell chemotactic assay. For scratch wound healing, confluent cells were serum starved overnight and scratched with a P200 Gilson pipette tip. The cells were kept in the presence of culture medium without FBS, or endothelial cells condition medium after scratching. Six fields at fixed location were visualized at indicated time-points after scratching and assessed the wound closure rate using software Image J.

For transwell chemotactic assay, cells were placed on the upper layer of polycarbonate membrane filters with 8- μ m pores (Corning Inc, Corning, NY or Falcon 353097) and culture medium or EC condition medium was placed in the lower chamber below the cell permeable membrane. The number of cells that have migrated through the membrane were stained by crystal violet staining solution and counted following 8-hour incubation. Each experiment was duplicated, six randomly selected fields of migrated cells were photographed and counted.

RNA Extraction and Real-Time qPCR for gene expression

The femoral artery was flushed with Trizol by a 29-gauge insulin syringe to isolate EC RNA. Lung ECs were isolated by magnetic separator following incubation with anti-CD31 antibody conjugated Dynabeads (Invitrogen, Carlsbad, CA). Total RNA from femoral artery or lung ECs and cultured cell line were extracted by

Trizol (Invitrogen, San Diego, CA, USA). Reversed transcription was performed by SuperScript First Strand Synthesis System (Invitrogen). Quantitative real-time polymerase chain reaction (qPCR) was performed using SYBR Green Supermix. Expression of genes was quantified with primers listed in Table S3.

EC RNAs from arch and thoracic aorta, lung, and from culture cell lines were extracted by TRIzol and cDNA was synthesized by SuperScript First Strand Synthesis System (Invitrogen). Real time qPCR was performed using AceQ Universal SYBR qPCR Master Mix (Vazyme Biotech Co. Ltd) in an ABI 7500 Real-Time PCR System (Applied Biosystems) with housekeeping gene β -actin or GAPDH as a control. Primers used for quantitative real-time PCR were included in Table S3.

Western blot

Proteins were extracted and separated on SDS-PAGE gels, transferred to PVDF membranes and blocked with 5% milk following incubation with primary antibodies against Foxp1⁴⁹, MMP9 (Proteintech, 10375-2-AP), Cdkn1b (Servicebio, GB11154), GAPDH (CST, 2118). Bound antibodies were detected by a peroxidase-conjugated secondary antibody, and the signals were visualized using a chemiluminescence kit (Cell Signaling Technology).

Chromatin immunoprecipitation (ChIP) assay

The chromatin DNA was made from lung ECs for investigating the association of Foxp1 with MMP9 and Cdkn1b gene using a commercially available kit (Millipore, Catalog No. 17-295) as manufacturer instructions. Briefly, the lung ECs were fixed with 1% formaldehyde, neutralized with acid glycine. Nuclear lysate was sonicated to 200 to 500 DNA base-pair fragment size and immunoprecipitated with the Foxp1 antibody as well as control rabbit IgG. Samples were cross-links reversed via incubation with NaCl and digested with Proteinase K and RNase for DNA isolation, DNA was subjected to PCR using the primers listed in Table S4.

Luciferase Reporter Assay

Cells were transfected with pGL3-promoter of the firefly luciferase reporter vector containing Foxp1 binding sequence of the promoter of MMP9 and Cdkn1b gene. Luciferase activity was determined and normalized to the corresponding renilla-luciferase activity in cell lysates using Dual-Luciferase assay kits (Promega, Madison, WI, USA)⁵⁰.

MMP activity assay

The MMP activity was determined using an assay kit from Abcam according to the manufacturer's protocol. Briefly, 5×10^5 cells were seeded into 6-well plates and allowed to attach overnight, then starved with serum-free media for another 12 h. Cells were stimulated with 10% FBS and 50 μ l of medium was collected at 1 hour following FBS stimulation. The medium was mixed with 50 μ l of 2 mM APMA working solution and incubated for 15 min at 20°C followed by addition of 100 μ l of the fluorogenic peptide substrate solution in the kit. The MMP activity assay was measured by microplate reader at the Ex/Em = 490/525 nm.

Lentiviral package

Lentiviral package was performed using lentiviral packaging vector pCMV.DR8 and pMD2.G (Addgene, Plasmid #12259) in human embryonic kidney (HEK) 293T cells (ATCC, CRL-1573). The viral supernatants were collected 48 and 72 hours after plasmid transfection, and the viral titer was determined by RT-qPCR.

For knockdown of MMP9 expression *in vivo*, viral supernatant was concentrated by ultra-filtration (100 000 MWCO, Centricon Plus-70, Millipore) and 10^9 IU (integration units) of lentiviral-MMP9 shRNA per mouse was applied to the injured segment in the presence of 10 g/mL DEAE-dextran for 20 minutes after wire injury. The

infection efficiency was assessed by immunoblotting using a MMP9-antibody (Proteintech, 10375-2-AP). For knockdown of Foxp1 and MMP9 expression *in vitro*, the viral supernatant was applied to HUVECs in the presence of 8µg/ml polybrene (Santa Cruz Biotechnology) and the infection efficiency was confirmed by RT-qPCR and western blot.

Data S2. Two-way repeated-measures ANOVA for cell number and MTT activity

Table S1. RNA high-throughput sequencing results of *Foxp1*^{ECKO} mutant and littermate wild-type fluorescent reporter mice.

Symbol	Gene ID	WT	Foxp1 ^{ECKO}	Log2Fold Change	Full Name
Mmp11	17385	1.31	1.47	0.17	matrix metalloproteinase 11
Mmp12	17381	0.36	20.16	5.80	matrix metalloproteinase 12
Mmp13	17386	0.27	5.10	4.26	matrix metalloproteinase 13
Mmp14	17387	20.46	54.48	1.41	matrix metalloproteinase 14 (membrane-inserted)
Mmp15	17388	12.58	10.91	-0.21	matrix metalloproteinase 15
Mmp17	23948	1.16	0.45	-1.38	matrix metalloproteinase 17
Mmp19	58223	2.92	14.94	2.36	matrix metalloproteinase 19
Mmp2	17390	13.18	8.29	-0.67	matrix metalloproteinase 2
Mmp24	17391	2.71	1.79	-0.60	matrix metalloproteinase 24
Mmp25	240047	0.55	3.96	2.86	matrix metalloproteinase 25
Mmp28	118453	31.88	8.84	-1.85	matrix metalloproteinase 28 (epilysin)
Mmp3	17392	2.63	0.89	-1.56	matrix metalloproteinase 3
Mmp8	17394	16.26	44.05	1.44	matrix metalloproteinase 8
Mmp9	17395	5.81	36.96	2.67	matrix metalloproteinase 9
Cdk1	12534	0.17	1.94	3.53	cyclin-dependent kinase 1
Cdk10	234854	8.82	5.92	-0.58	cyclin-dependent kinase 10
Cdk11b	12537	23.50	17.89	-0.39	cyclin-dependent kinase 11B
Cdk12	69131	8.69	9.11	0.07	cyclin-dependent kinase 12
Cdk13	69562	9.78	9.43	-0.05	cyclin-dependent kinase 13
Cdk14	18647	44.91	23.91	-0.91	cyclin-dependent kinase 14
Cdk16	18555	31.63	19.47	-0.70	cyclin-dependent kinase 16
Cdk17	237459	19.93	21.62	0.12	cyclin-dependent kinase 17
Cdk18	18557	1.50	1.46	-0.04	cyclin-dependent kinase 18
Cdk19	78334	15.33	42.45	1.47	cyclin-dependent kinase 19
Cdk2	12566	9.49	10.26	0.11	cyclin-dependent kinase 2
Cdk20	105278	2.82	2.93	0.06	cyclin-dependent kinase 20
Cdk2ap1	13445	67.82	48.30	-0.49	CDK2 (cyclin-dependent kinase 2)-associated protein 1
Cdk2ap2	52004	26.49	48.96	0.89	CDK2-associated protein 2
Cdk4	12567	45.37	38.62	-0.23	cyclin-dependent kinase 4
Cdk5	12568	7.89	8.48	0.10	cyclin-dependent kinase 5
Cdk5r1	12569	0.70	1.85	1.40	cyclin-dependent kinase 5, regulatory subunit 1 (p35)
Cdk5rap1	66971	9.93	4.78	-1.05	CDK5 regulatory subunit associated protein 1
Cdk5rap2	214444	1.70	2.30	0.44	CDK5 regulatory subunit associated protein 2
Cdk5rap3	80280	8.44	13.62	0.69	CDK5 regulatory subunit associated protein 3
Cdk6	12571	1.97	4.01	1.02	cyclin-dependent kinase 6
Cdk7	12572	5.39	3.72	-0.54	cyclin-dependent kinase 7
Cdk8	264064	7.14	8.83	0.31	cyclin-dependent kinase 8
Cdk9	107951	12.36	15.14	0.29	cyclin-dependent kinase 9 (CDC2-related kinase)
Cdkal1	68916	6.21	3.45	-0.85	CDK5 regulatory subunit associated protein 1-like 1
Cdkl2	53886	1.69	2.15	0.34	cyclin-dependent kinase-like 2 (CDC2-related kinase)
Cdkl5	382253	1.33	0.68	-0.98	cyclin-dependent kinase-like 5

Cdkn1a	12575	536.79	144.95	-1.89	cyclin-dependent kinase inhibitor 1A (P21)
Cdkn1b	12576	51.14	36.69	-0.48	cyclin-dependent kinase inhibitor 1B
Cdkn1c	12577	8.03	3.91	-1.04	cyclin-dependent kinase inhibitor 1C (P57)
Cdkn2aip	70925	10.49	7.44	-0.50	CDKN2A interacting protein
Cdkn2aip nl	52626	24.26	14.33	-0.76	CDKN2A interacting protein N-terminal like
Cdkn2b	12579	4.86	2.76	-0.81	cyclin-dependent kinase inhibitor 2B (p15, inhibits CDK4)
Cdkn2c	12580	5.72	3.84	-0.58	cyclin-dependent kinase inhibitor 2C (p18, inhibits CDK4)
Cdkn2d	12581	15.05	13.26	-0.18	cyclin-dependent kinase inhibitor 2D (p19, inhibits CDK4)
Cdkn3	72391	0.36	1.69	2.24	cyclin-dependent kinase inhibitor 3

Table S2. Sequences of gene-siRNA and shRNA.

Gene Name	Sequence
Human	
Scramble	TTCTCCGAACGTGTCACGT
Mouse Cdkn1b siRNA	GGCCAACAGAACAGAAGAA
Human Cdkn1b siRNA	GGCCAACAGAACAGAAGAA
Mouse MMP9 shRNA	ATTCTTCTGGCGTGTGAGT
Human MMP9 shRNA	GCGTGGAGAGTCGAAATCTCT

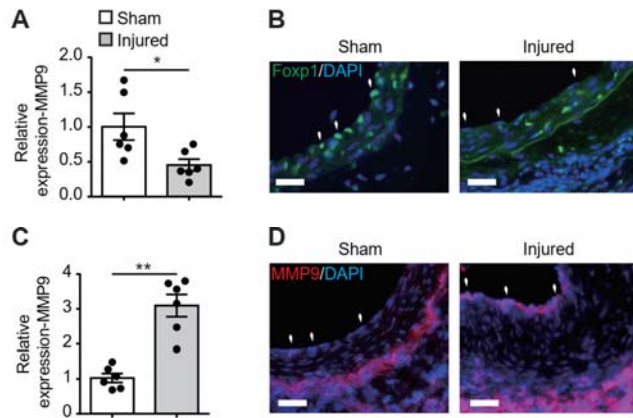
Table S3. Primer sequences for reverse transcript quantitative PCR (RT-qPCR).

Gene Name	Primer Sequence
Mouse	
<i>Foxp1</i>	Forward: 5'-AAGCAGCTAACACTAAACGAAATC-3' Reverse: 5'-TTCCACGTGGCTGCATT-3'
<i>MMP9</i>	Forward: 5'-TGTATGGTCGTGGCTCTAA-3' ^{f1' sEP: 3'} Reverse: 5'-GTGCTGTTCGGCTGTGGTT-3' ^{f1' sEP: 3'}
<i>Cdkn1b</i>	Forward: 5'-CACCAACGCCAACTTCCT -3' Reverse: 5'-GCTTCTTTCGCACAATCTCA -3'
<i>Gapdh</i>	Forward: 5'-AAATGGTGAAGGTCGGTGTGAACG-3' Reverse: 5'-ATCTCCACTTTGCCACTGC-3'
Human	
<i>Foxp1</i>	Forward: 5'-CTCCTCCTCTGCACCTTC-3' Reverse: 5'-TGCTCCTCATGGGACAAA-3'
<i>MMP9</i>	Forward: 5'-TCCCTGGAGACCTGAGAACC -3' Reverse: 5'-GCCACCCGAGTGTAACCAT-3'
<i>Cdkn1b</i>	Forward: 5'-TACGAGTGGCAAGAGGTG-3' Reverse: 5'-CGGATCAGTCTTTGGGTC-3'
<i>GAPDH</i>	Forward: 5'-ATGGAAATCCCATCACCATCTT-3' Reverse: 5'-CGCCCCACTTGATTTTGG-3'

Table S4. Primer sequence for qPCR of chromatin immunoprecipitation (ChIP) assays.

Promoter	Primer Sequence
<i>MMP9</i>	Forward: 5'-GCATAGGCAAGCAAGTCT -3' Reverse: 5'- TGTTGTGGTTTGAGGTGG -3'
<i>Cdkn1b</i>	Forward: 5'- CTGTCTGGGACGGCTCTA-3' Reverse: 5'- CCGCTCTTATCAGGGTGT-3'

Figure S1. Foxp1/MMP9 expression in endothelium of sham and injured femoral arteries.



A-B, Foxp1 expression in endothelium of sham and injured femoral arteries by qPCR (A) and immunostaining (B). **C-D**, Expression of matrix metalloproteinase-9 (MMP9) in endothelium of sham and injured femoral arteries by qPCR (C) and immunostaining (D). Data are means \pm S.E.M. * $P < 0.05$, ** $P < 0.01$. Scale bars: B, D 100 μ m.

Figure S2. Sequence analysis of MMP9 promoter.

A

MMP9 Promoter sequence (-5 kb to translational starting site)

```
AGTTGGTAAGAAAGAACAGCAGCAATCCTGAAGGCGAGTGAAGTGGTACCCACTGCTTACCCACTGTTCCAGGCACCTCTGTAACAGGCCACATGGG
AAACACTGTTATTAGCACTTGTTTTAAAGTGGGGAAATGGTAGTGTGTGCTGATAGCTGGGGTACACAAATGAGCTGAAGCTTGGATTCGGCAGTCC
AATCCAGAGTGGGAGCCCCATTGGCCACTCACTCTGCTGCCCAAGTCTGGCCCTCTGCTGAACCTGTTCCACATCTGCATGACGAAAGGAAATAGA
ATAGATGGGGACACCTCCATGTGGTGTATTCTGTGACTCTTTTTTCTCCCCAAATTTCTACCCAGTACAGCAAGTACACTTTTAATACTAG
TATTCAGAAGGCATAGGCAAGCAAGTCTGAGTTTGAAGTCAGCTGATCTACACAGTGTGTTCTAGGCCAACAGAGTTCCTAGTAAGACCCACCTCA
AACCACAACACACACACACAGCCCCACTATGCAGGAACATACACATACATGCAACATACATACATGTAGATACATGTAGGAGCACACATATACATA
CATGTATACAAAGCATTTCACACGTGAGCACACCCTTGCACACACACATGCAAAATGCACACACACCCTGTACTGCATGTCATCTTTATGTGTTTTTATGG
GATTGTATGACACAGTGTCTAGAGGTCAAGGGACAACTGTAAGAGCTGGTCTCTTACCATGTTAGTCCCTGGGATGAACCTAGCTCCTGGTGTCT
TGGTGACAATCTCCTTAACTGCTGAGCCATCTCACTGGCTCTCTGGAACCTGACTTAAAGTCTAGCTCAGAAACAAAGAAAGTGGGGAAGGAGGAGG
AAGAAAAGGAGAAAAGAAAGCTAGGATCTTAAAGTAGCCCAAGCTGGCTTGAACCTGTATGCAACCAAGGATGATCTTAGACTCTGACCCACCTTCTC
TGACACCTGAGGACATAGCACACTTCTAGCATAATGCTTAGCTGTGAAACTCAACAAAAATCTGTTCAATAGCTTGTGTTTGTGTTGTTGTTTT
TCGAGGCAGAGTCTCTGTCTAGCCCTGTCTATCCTGGAACCTGTCTGTAGACAGGCTGGTCTTGAACCTACAGAGATGCACCTGCCTCTGCCTCC
TGAGTGTCTGGGATTAAGGCATTTGCCACCACAGTGGAGGCTTATTATTGTTGTTGTTGTTGTTGTTTATTCAATAGAGGGTCTCAGCAGCCCA
GGCTGGCCCTCAAACCTGCCAAGTGTAGGGATTGGCTTTGAACTCTCTCCTCTTGTCTTCACTTCCAAAGTGTGGTGGCCTAAGTTGAAACAGTCAT
CAAAGATGTGAAGATCTAGCTGGGTGGTGGTGGTGCACACCTTAAATCACAGTGTCTGGGAGGCAGAGGCAGGTGGGTCTCTGAGTTCAAGACCAGTCT
GGTCTACAGAGAGGATTCAGGACAGCCAGGACTACACAGAGAAACCTGTCTTAAACAAAAACCAAGCAACCAAGCAAGGACCAACAAATAAAAAAT
TGAGCATCCTCACTAACGGTTGAGTATTGATGAAACTTTTGAGCATTATAAAGAAAACTCAACACACACCAGAGGCTCTCTCTCCACTCACCA
GGGAACATTTGGTAACATCAATGGTGTCAATGGTATGGTGGTGTCTGCTGGCACTAGGAGGAAGGGAGGGTGGGACACCTTAGACACTGC
AGTGTCTGGGGACATCCCAAAACAAAGGACACAGCCCAAGGATAAAGATGCCAAGCTTGTATGATGTGGTGGGGATCTTAAATCCCATCACTCAGG
AGGCAGAGGCAGGGGGATCTCTATGAGTTGGAGGCCAGGCTGGTGCACACAGCAAAATAGGCCAGCCAGGCTCCATAGTGGGACCCTGCCTCAAA
AACAACCAAGGGGTAGAGCTCAAGAAACAAGACATACATAGATGACATGATGATAGATGTGGCATACTGCATAGATGTGGCATACTAACACAGAC
GAACACACCACATAGACATGACATGGTATAGATGTGACATACTGCATAGATGTGACATCTAACACAGACTGGACACACCAGTAGACATGACATATATGTA
CATACAACACAGATGACATATGGCAGATGTGACATATAACAGATGTAACATACCATACAGATAGGACATACATACATACATACATAGATGTGACA
TATAACAGAGCCATGGCAGATAGTGCATAGACATCACATCCACATGTTGACGATCCTTAAAGCAGTGTCTGGCAAGATGGGAATACTGCATAGATTCCTCTGAA
GTTCTTGTCTGACCTCGATGAAGATCAGGATGGGAGGCTCTTATTTGTTCCATTCAAATCTGTATTAGTCTTTGGCCCCACAGTCCAGGCTCTG
TAATATGGTTACCCTGGGACCCTGTCTTACGATGTGACCCCTCAAAGTCTGACCTCCAGCCTTATCGTACTAAGGTAGCAGGGGAGAGAGGGGTT
AGGTGGCAAAAGCCCTGGAAACCCACCCATTTCAATCACTGTACTCTGATCCGCTCCCTGCCACAGCAGATGAGAATCTTGTACCCTGGCTCTGTGGT
TTTTTTTGGTTTTTGTTTTTTGGAGACAGGGTTCTCTGTATAGCCCTGGCTGCTGGAACCTCACTTGTAGACCAGGCTGGCCTGCAACTCAGAAATC
TGCCCTGCTGCCTCCCAAGTGTGGGATTAAGGCGTGCACCACATGACGAGGACCTGAGATCATGGGCAAGTCCCTGACTGCTGAGTTG
AAGTTTCTATTCCAGAAAAGCCAGAGTTACCTCCCAAACTAACCTTGTAGCCAGGCATAGTGTGCACACCTATGACACAGCGCTTGGGAGGCAGAGGC
AGGGGATGGGAGTTCCAGCACAGCCTGACTTCCAATTTGACTTTGTCTCAATAGATGGAGGGTGGGTGGGGAAATGGCCAAGTGGGTCCAGAGCATT
ATTGTAGAAAGCAGGAGGCCAGCTTCCGAGCTACAACATCCACGTAACAGCTGGGTGGCAGCCTACTTGTCTCACTCCAACTGACACAGATGGAGA
CTCTGAGACAGGGTTACCAAGGCTTGTCTGGCGCCAGCCTGGCTGCAAACTCCCTGGGCTCTAAGTTTAGGGAGACTCTGCCTCAAAGGAAACAAAAG
AAGATGACAGAGGGGGACAGCCAACATCTCCTCTTGCCTTGGCAGTCTGGATGTGTGTCCTGACACACACATATGACACACACACACAAACACA
CACACACACACACACACACACACACACACACACACACACACACACACACACACACACACACACACACACACACACACACACACACACACACAC
CTCAGTTGAGAGTACTTGCCTAGCATGTGTGAGACCCTAGAGGCTTGGGCATACACACACACACACACACACACACACACACACACACACACACAC
CACACACAGTCTCACACATATGGATAGCAATATATAGGAGAGTTTGTAGAGCAGTATGACACACACACACACACACACACACACACACACACACAC
GCGCCCTGGAGGTGAATGCCTTGGCCAAAGGTGGTGGGAAATGACGAGGTTGGGAAATGGTAGACCAGAACTGCAATTCAGTGTGGAGCTCACCA
GTGAGAAAGCATTAAGAGAAGCTTGGGAGAACACCCAGCTCTCTCTCCGGCTCACAGGCTGTTGTTGGGAAGCAGATGAAGGCTGGGACACACA
GGAGGCTTAGTCAGAACAGCTTGTGTAAGACAGATCAAGGCCCTGCTCCACCATGGTGGCAGGCAGGAGGATGGAAGGCTGGGGGCTGCCGGCTG
TTGGCAAGACTGTGCCAAAGCTTCTGAGTGGAGCAGGCGAGGCTGGAGGAGGGGAAAGGTTCCATGACGATCTCACAGCTCGGGAGAGGAAGGT
GTTTGGCCCATCCAGGTCACCCCAAGGCTTAGAGCCAAAGCCAGTCTCCTAATTTCCAATCACAACTGACACCATCACTGAGGTTCTGTGAAACAC
TGCTGAAAGTGGTTTTCTGTGTTTCGAGAGTCTCATTTTTATCTCAGATCAATATAGGGGACAAAGGCTTGGAGCAGAAAGGCTGTTTTTGTCTTAAA
CAGAAGAGGAAAGGATAGTGTAGCTGAGAAGGATGAAGCTTCTGCTGCTCCACATGTGTGTGTCCTCCCGCCCGCCAGGCTCATCTTCTTCCCC
AAGGAGTCAAGCTGCTGGAGCTAGGGGTTGCCCATGGAATCCCCAACTCTGCCTCAAAGAGCCTGCTCCAGAGGCCAGGAGAGGAAGCTGAGT
CAAAGACTCTATCAGGGGGCGGGGATGAGAGGATAGAACCACAGTGTGGGATGGGCTCCAGGCTGCACTCTGGCCAGGGAGGGGTTGCTCAGAA
GCCAAGGAAAGAGGGGCTCGGGCCTCAGGCTCCTCACTTTTACTGGGCTGATCAGTCAAGGCGCTCAGACCTAGGGCTAGGTGAATGCCCCATCC
TGCACACCCTCCTTCCCTTTCCCAAAAGTCTGCAATTTGCAGAAACTAAACCTGAGTTCTGTGGTTTCTGTGGGTTCTGTGGGCTGGGGGCTGCTG
GCAATGGGGACTGTGGCAGGCATAAGGGAGGGGTTAGTGTAAACACACACACACACACACACACACACACACACACACACACACACACACACAC
CTGAGTCAAGTAAAGCTGGAGGGGAGGGGCGGGGCTACTGATCCGTTTACTGCCTCTTAAATCTCTGCAAGGCAGCGTGTAGCCAGAAGCTGCG
CTCCTCACCATG
```

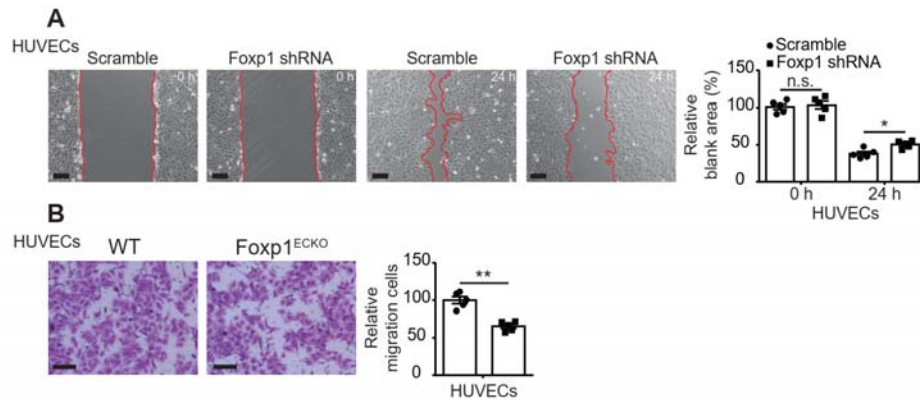
B

MMP9 Promoter cloned sequence (-4.7 kb to -3.7 kb before translational starting site)

```
GCTGGCTTAGAAGTCTGATGCAACCAAGGATGATCTTAGACTCCTGACCCACCTTCTCTGACACCTGAGGACATAGCACACTTCTTAGCATAATGCTTA
GCTTGTGAAACTCAACAAAATCTGTTCAATAGCTTGTGTTTGTGTTGTTGTTTTCGAGGCAGAGTCTCTCTGTCTAGCCCTGTCTATCCTGGA
ACTCGTTCTGTAGACCAGGCTGGTCTTGAACCTCACAGAGATGCACACTGCCTCTGCCTCCTGAGTGTGGGATTAAGGCATTTGCCACCACAGTGGAGG
CTTATTATTGTTGTTGTTGTTGTTGTTTATTATAAGAGGGTCTCATGCAGCCAGGCTGGCCTCAAACCTGCCAAGTGTAGGGATTGGCTTTG
AACTCTCTCCTCTTCTTCACTTCCAAAGTGTGGTGGCAGGCTAAGTTGAACAGTCAAAAGATGTAAGATCTAGCTGGGTGTGGTGGTGCACACC
TTAATACAGTGTCTGGGAGGAGGCGAGGCTGGTCTGAGTTGAGAACAGGACTGGTCTACAGAGAGATTCAGGACAGCCAGGACTACAC
```

A-B, matrix metalloproteinase-9 (MMP9) promoter from -5 kb to translational starting site has 6 Foxp1 binding sites (A) located in the promoter region -4.0 kb to -3.5 kb, which is cloned to pGL3 luciferase reporter vector (B). The Foxp1 binding sites are indicated by red font, and the translational starting site is indicated by green font.

Figure S3. EC-Foxp1 deletion reduces cell migration.



A-B, Knockdown Foxp1 in human umbilical vein endothelial cells (HUVECs) displayed decreased cell migration, shown by wound healing (A) and transwell assays (B), with representative images (left) and quantification data (right; n=5). Data are means \pm S.E.M. *P<0.05, **P<0.01 and n.s. not significant. Scale bars: A, B 100 μ m.

Figure S4. Sequence analysis of Cdkn1b promoter.

A

Cdkn1b Promoter sequence (-5 kb to exon1)

```
TTTATGCCTGCAGCCAGAAAGAGGACACCAGGTGTCCTTATAGATGGTGGCTTCCATCTCTAGTTCTTGTGTGTGGCTGCCTGCCAGTCAAGTGAT
ATGCTCCACAGGCAAGAGCTGAGATTTAGTCACTCTTAATCCCCACAGCTGCTGAAACAAATGCACTGGGAATTTTCGCCACGGTAAGGTCAGATC
CTTCTGCTACTTACCCCTCTGGTGTCTGGTCTTTCCCTTACCTCTTGTCTGTAACAGCTGCATTCTGAGGCCCGCCGGTCCAGTGTGAGTTGATGCTC
CTGTGGATACTCTCCCTTCTTGTCCCTGTCCACAGGTGTCCTTTGACTGCATCAGGCAAGCTCCACCCAGAGCTTTGCGACTCCCTCTTGTAGTTAC
TGGGCCACACTCTTCTCAGACTTGGCATGCTGTTTTCTCAAGCCCTCAGGCCTCTGTGAAAGCCACTTTCCCTGGCCACAGTGTAGCCCTTTCC
ATCACTTTCCAGTTTTCCATTGTTGCTCTCCAGAGTGTCTCCCTTACACTACCTTGTGTTACTTAGTGGTTATCTTCTGTCCCTCCCTCTCTTACTA
CAATGAAACTGCAACTTAATTTCCATCCCGAGTACCCAGGATAAAGCCTCCTTTATTGGCGATGCAATACATACGGAAGGGCAGAAACAAGCTATG
TGGTCATATCAACCTATAACCCAAAGGCTGAGGCAGGAGGATTGCAGCACATTCAGACCACCTTGGATTACACACGAAACGCTTCAAAGCAACAAC
AACAAACAAACCCAAACAAAGAAAAACCAAAACAACTCCCCACAGAAAGAAACAAAGTAAATGGAGAGAAACACTGCAGTTGGTAGGGAGGTCCACCTCC
ATAATCCTAGCATTCAAAGGGGAAAGAGAGGCAGGCACAGAGGCTGAGGCAGAAAGGAGGCCTGTAAGGCAGCCGAAGCTACAGGGTGTAGTTTCAGGA
ACCCGGCTGGGGTGAAGAGGGGTAGGGGTGGGGCGGGGACACTAGGCAAGAAAGCAAGCAGCAGCAAAAAAAAAAAAAACAAACAAACAA
AAAAAACCAAAACCAAAACCCCCAGCACGTTAACTCGAAGGACACAGTAAATATTATTAAGTTGAATTAAGTGTGAGAACAGGGCACGCCTTCC
CCGGCTCAAGAAATAGGCAGTTGAAGAGATTGGGGGTAGGAGTGAAGTTGCTGCTTTGATGGGTTTGGTGGGAGGGGTGGGAGGGCAGCGAG
ACTGCTCTTACAGCAAGTTGGGGCTATAATTGCCCTAGGAGAGATGCACACTGGGAGCCGGGCTGCTGGGAGCCACTTGCCTGCCACCCGTTGG
GACACTTATCTCCACGCAAGGTGTTCAATTTGTTGGTCTTCACTTATCGCTAAACTCAAAGTCTCAGCACTCGGGGAAAGGGGTGGAGGTGGAGG
GTGTTGCATGAGTGACACTTCTCAGAGCTATGTAAGAAAGCACCCGGAGTGGAAAGATGACCAAACCTTACAAGGACTAGGGGGTCTTGGAAAGCA
AACTTTGATGAAGGGCAGTGTGTTGGGACTTTATCTTCTGCCCTGAGAAAATTTTCCCTGGTTTCCCTTTCCGCAAGTTAAACCTTCAACAA
GGGACTGTGCTCTGGATCTCCGCTCCTTCTTCAAACTCCATAGTATTTTTTTTCTTTTTCTTTTTTCCCTTTTTTACGCATCGCTGCTACAGTAGGGC
CTGCCTCTGGTATTGCTCCGATCTTGGGTGCTTGTATTGTAACAAACACTTTAGATCGGTAGTGAGTCCGCTCACTTCTATCATATGTTCTGG
CAGCCAGACTTCTAAGGTGGAGCGCCAGGACTGCTATACATGTGGGATTAACAGATCAACAAAATGGTGTCTCTGCACAAGGCTGAGAGACTCCGGC
GGTGCAGGGACAGAAAGTTAACTTTCTGCTTTCATACAGACATATCGTGATGAATAAAAAACCTTCTGAAAGTGGATTGAATTTCTATTTTACATA
AGAGCTATAGTTACACAGAAAGAGGAGGAGGAGCTCCTTGGCTAGTATTGTTCTTTAGTTAATATTTGAGACACGGTCTAGATAGCTCAGGATG
GCTGTGAACCTCTGTGTAGTTGAGAAGGACTTTGAATTCCTTACCTCTACAGTATGATCATCTAGCAATTTAAATGTTTATGGTGTGGTGTCAAGG
CTGGGCATATACCGGAGACATAAGGCTCACCCATTTTACTGTGTTTTCTTCCAAAGTTCAGTAACTAAGTAGGTATGATAGATATGGGGGAGGGGCA
CAGCTGGGAGACTGGTGAAGTGGTTCATGTTGAGTGGTGCAGACACTGCCATACAAAGTCCGCAACCTGAGTTCAAGCCGCAACCTTCAAAATGTTGT
GGGGGACCTGATTCAACGTAGTCTCTGACCTGAGCAGACATGATGCCATGACGAGTTTGTCCACATATGTCATGTCATGCACAAACATTTGCAATAAT
TTTTCAATATAGCGTGTGTATATATGTATGAGTAGGTAGGTACAGAGTCAATAGTACACCTACCAAGAGGAGTCAACTCGCTCTATCATATGTTCTT
GAAAACCTGACCTCAGCATGTGAGGCATTTTGGCAGGCACCTTACCTGCTGAGCCATCTTAGCCCAATCTCAAAAAACCAAGACAACCTGAACACAG
TGGGGTGGACCCATAGTCCAGTGAATTTTGTGTTTTCAGATACAGAATCTCCTGTAACACAGTCTGGCCACCAACTCAGCTATGCAAGTCAAGAAATGAC
AAATTCCTTCTCTTGTGTTTGGTGAAGCTAGCTACTGAAGCTGAGGCAGAGCCAGGAGTTCAAGGCCAGCCTGACCAACACAGTGCAAAACCA
CAGCAAAACAAAGCACCAGAAAGAGGCAACTCCCACTTGTGCCAACTGAACAGTGCAGAAAGGCTGGATTGAAGTCCACGCCTGGATGCTGCT
TCTTCTACTCAATGAGCCCAACCATTTTTGAAATCTGTATTTTCAGCTGAAGTATGATAGTATGATACCAAGGCTTGTGACAGCTGCATTTGATGAT
CAAGGAGACATCTGTGGGATCCAAAGGCTGGAAAGAGACCTTTTGGATCCTTGTAAAGAGAGTAGAGTCTGCAGACTGCAACCCATCCAAATCCAGACA
AAATCAGGAAACACTGAGACCACAGAAAGAAACAGACAAAACCAAAACCGGAGAAATGAGGAGACTTGCACCACCTGAATAGAAAGTCCCGCAGACA
GAAACCTGAGTAACTAAATTTCTCATTGGTAAAAAGAGGCTAAACCTTAAAGAACTTCTGGACTTTACATTTTGAATGAGGAGCAAGGCAACAC
ACACACACACACACACACACACACACACACACACACACACACACACACACACACACACACACACACACACACACACACACACACACACACATCCTGG
CAAGATGTGGCTAAGAAAAAGTCAATATTCAGTCTCACCTACACAGGAAAGATAGGAAAAACATGCTTCTTTGGGACACTAAACAGAAATTTAATT
TCCCTAAACTGGTTTTTGTGTTTGGCGCAACCAAGACTGTTGGGAATACTAGTGGGCAAAAGCCCTTAAATCTCACTGAACCTGACATACGACAGGCT
GGCTATTCTGTTTAACTTCTGTCAGTGTGCTCAGCAGTATAGAGAAATGTGAAGTTGCCAAAGGAGCTGAAAAAACCCACCAACATTACTAGATT
GGTAATACCGTGGTGGTATTATAATCACTTGAATCTAGTCTTAGATCCTTAGGAAAGTGTTCCTGCCCCTTAAACACCTGCAGCTCTTAAAGTAT
TTGCTTTGTAATTTGTAATTTGACTGAGTAGGTTGGAAGCAACAGGCTGGTGGGAGAAAAAGAGAAGGAAGGCACTGTTGAGTTGGCCTCGGACTCAG
GTGGAGGGAACGGCTTCCGCCGGGAAAGACATAAGGGTATAAGGGCAGTTCACACAGCTATAGCAATGGCTTCACTGTGCTTAGGAAACCAAGAAA
ATCAGAACTGGCTTTTGTGTTTCTGCTGGGACGGCTCTAAAGACGGCTTGGGAGAGCACTGGGGGTTTTCAATCTCGAGACTCGGAGTGGGCGGAGC
GCTTGGATTGAGAAACCCCTGATAAGAGCGGTGCTGCTGCTTCTTTTGAACACCTCCTGGCCTGCTACATAGCAGAGACTTCTGGGGTCAAG
GCTAAGCGCGGATTCGCAACCCAGCTAAGGCACCCCTGCGGGTGGGGTGGGTGGCTGCCCCAGGCCCTGAGCCAAAGTTTCTGAATCTCTCG
CATACCCTCCTCCTTCCACCTCGCGAATGCAAGTGGGCTGAACTAGCCACCGAAGCTCCTAATAAGCCGCAAGCCAGCTAGGAGCCCACTGGTCC
AGGCCCTAGGTTTTCGCGGGCAAGACCTGGAGTTCGAGTGGGAGCGGTGACGCGCCTGCCAGCGCAGCTCTGCAGCGCCGGGACCTAGATCCCC
GGGTCCCTGCTGGCCGCGGCTGGCCCTCCCACTCCTCGGCCGTTTGGCTAGTTTGGTTGCTTATTTAATTTTCCGGGGCCAGCCAGAGC
AGGTTTTGTTGGCAGTGTACACCTCCGAGTAGTCAAGGACCAAGCTGCTGCGGGCCTACGGGGAGGCGCGGCTCCGGGAGCGGAGAG
GCGGGCGCGCCGCGCCGGGGCCACCTTAAAGAGCGGCTGCCAGCCTGGGCGGAGCGGCTCCCGCGCCGAGACCAATGGAGCTCCTCTCTGT
TAAATAGACTTG
```

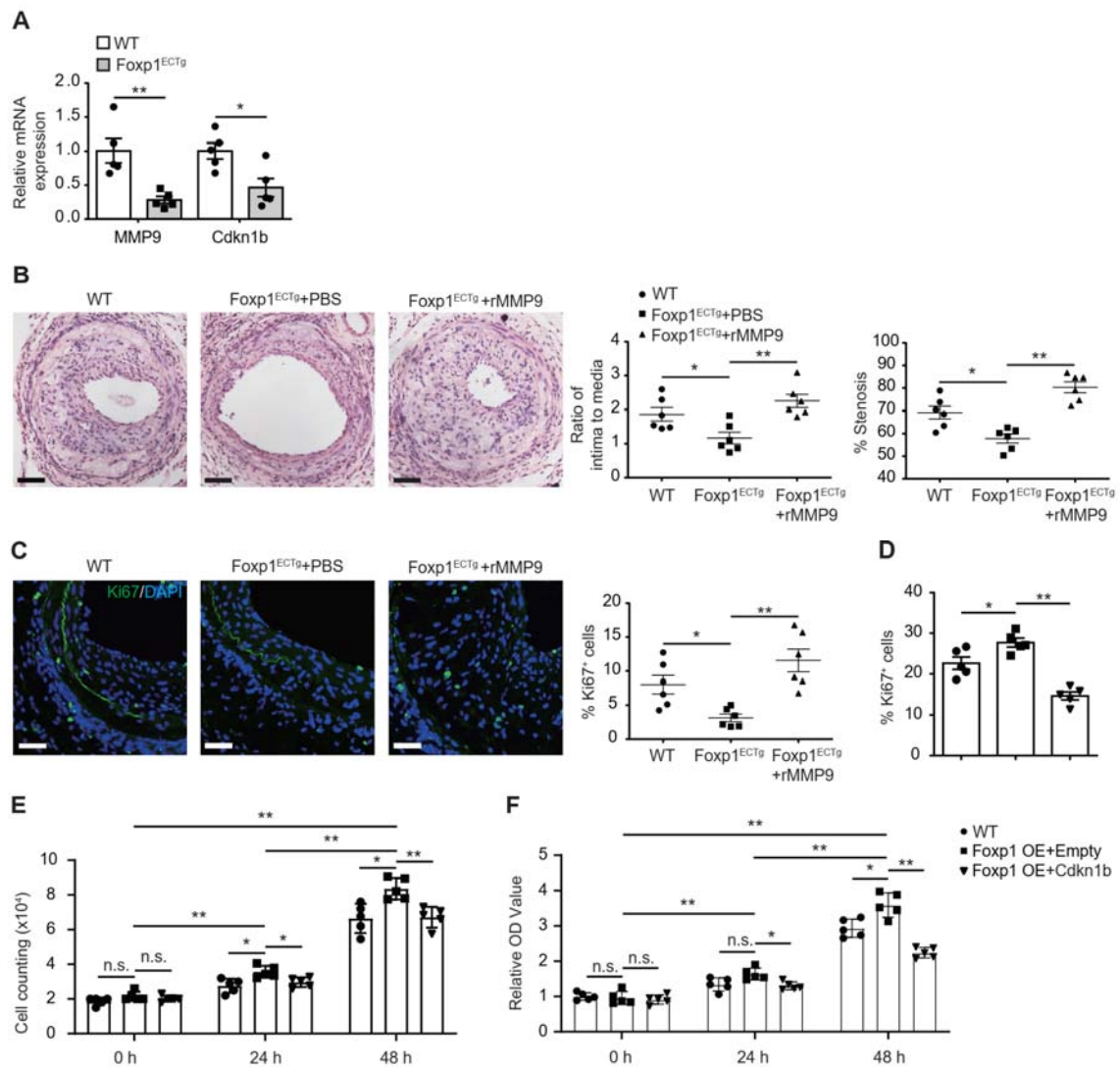
B

Cdkn1b Promoter cloned sequence (-1.4 kb to exon1)

```
GCAAGATGTGGCTAAGAAACAAGTCAATATTCAGTCTCACCTACACAGAGGAAAGATAGGAAACCATGCTTCTTTGGGACACTAAACAGAAATTTAA
TTTCTGTAACATGTTTTGTGTTTAGCGCAACCAAGACTGTTGGGAATACTAGTGGGCAAGCCCTTAAATCTCACTGAACTTCTGAGATACGACAGGC
CTGGCTATTCTGTTTAACTTCTGTCAGTGTGCTCAGCAGTATAGAGAAATGTGAAGTTGCCAAGGAGCTGAAAAAACCCCAACATTACTAGATG
TTGGTAATACCGTGGTGGTATTATAATCACTTGAATCTAGTCTTAGATCCTTAGGAAAGTGTTCCTGCCCCTTAAACACCTGCAGCTCTTAAAGAT
ATTTGCTTGTATTTGAATTTGACTGAGTAGGTTGGAAGCAACAGGCTGGTGGGAGAAAAAGAGAAGGAAGGCACTGTTGATGTTGGCCTGAGACT
AGGTGGAGGGAACGGCTTCCGCCGGGAAAGACATAAGGGTATAAGGGCAGTTCACACAGCTATAGCAATGGCTTCACTGTGCTTAGAAACCAAGA
AAATCAGAACTGGCTTTTCTGATTTCTGCTGGGACGGCTTAAAGAGAGGCTTGGGAGAGCACTGGGGTTTTCAATCTCGAGATCCTACGGTGGAA
GCGCTTGGATTGAGAAACACCCCTGATAAGAGCGGTCACTCTGGCTTCTTTTGAACACACCTCCTGGCCTGCTCATATAGCAGAGACTTCTGGGGT
AGGCTAAGCGGCCGATTCCGCAACCCAGCTAAGGCACCCCTGCGGGTGGGGTGGGTGGGCTGCCCCAGGCCCTGAGCCAAGGTTTCTGAATCTCT
CGCATACCTCCTCACTCCACCTCGGCAATGCAGTGGGCTGAACTAGCCACCGAAGCTCCTAATAAGCCGCAAGCCAGCTAGGAGCCCACTGGT
CCAGGCCCTAGTTTTCCGGGGCAAGACCTGGAGTTCGAGTGGGAGTGGGAGTGGGAGTGGGAGTGGGAGTGGGAGTGGGAGTGGGAGTGGGAGT
CCGGGTTCCCTGCTGGCCGCGGCTGGCCCTCCCACTCCTCGGCCGTTTGGCTAGTTTGGTTGCTTATTTAATTTTCCGGGGCCAGCCAGAGA
GCAGGTTTGTGGCAGTGTACACCTCCGAGTAGTCAAGGACCAAGCTGCTGCGGGCCTACGGGGAGGCGCGGCTCCGGGAGCGGAGAG
AGGCGGCGCGCCGCGCCGGGGCCACCTTAAAGAGCGGCTGCCAGCCTGGGCGGAGCGGCTCCCGCGCCGAGACCAATGGAGCTCCTCTCT
GTTTAAATAGACTTG
```

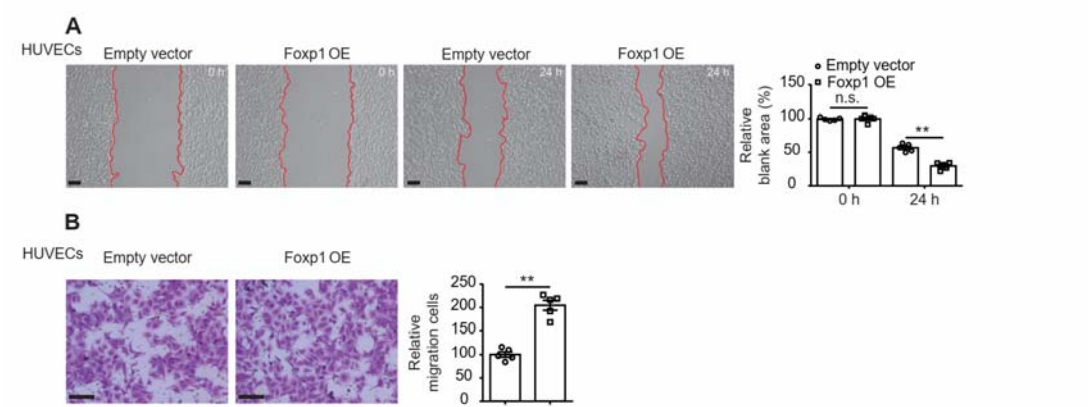
A-B, Cyclin dependent kinase inhibitor 1B (Cdkn1b) promoter from -5 kb to exon1 has 6 Foxp1 binding sites (A), and the promoter region of -1.4 kb before exon1 was cloned to pGL3 luciferase reporter vector (B). The Foxp1 binding sites are indicated by red font.

Figure S5. EC-Foxp1 gain-of-function decreases MMP9/Cdkn1b expression and MMP9/Cdkn1b protein reverses the EC-Foxp1-mediated decrease of neointima formation and increase of endothelial cell proliferation.



A, EC-Foxp1 gain-of-function mice (*Foxp1*^{ECTg}) exhibit a significant decrease of matrix metalloproteinase-9 (MMP9) and cyclin dependent kinase inhibitor 1B (Cdkn1b) expression in vascular endothelial cells (ECs) compared with wild-type mice by RT-qPCR (n=5). **B**, MMP9 recombinant protein reverses the decreased neointimal formation at 28 d after femoral artery wire injury caused by EC-Foxp1 gain-of-function, with representative images (left) and quantification of neointima area, intima-to-media ratio, % stenosis and media area (right) (n=6 for each group). **C**, MMP9 recombinant protein reverses EC-Foxp1 gain-of-function mediated increase of Ki67-positive cells in neointima at 28 d after femoral artery wire injury, with representative images (left) and quantification data (right) (n=6 for each group). **D-F**, Cdkn1b overexpression reverses the Foxp1 gain-of-function mediated increase of EC proliferation, shown by Ki67 staining (D), cell counting (E) and 3-(4, 5-dimethylthiazol-2-yl)-2, 5-diphenyltetrazolium bromide (MTT) assay (F) (n=5). Statistical values of cell counting and MMT are shown in online dataset. Data are means ± S.E.M. **P<0.01 and n.s not significant. Scale bars: A, B 100 μm.

Figure S6. EC-Foxp1 gain-of-function increases cell migration.



A-B, Foxp1 overexpression in human umbilical vein endothelial cells (HUVECs) increases cell migration, shown by wound healing (A) and transwell assay (B), with representative images (left) and quantification data (right) (n=3). Data are means \pm S.E.M. *P<0.05 **P<0.01 and n.s not significant. Scale bars: B, C 100 μ m.